



UNITED NATIONS
UNIVERSITY

GEOHERMAL TRAINING PROGRAMME

ORKUSTOFNUN



Gunnuhver hot spring at Reykjanes geothermal field

Luis Alonso Aguirre Lopez

MODELLING AND STABILITY ANALYSIS OF BERLIN GEOTHERMAL POWER PLANT IN EL SALVADOR

Report 3
November 2013



**UNITED NATIONS
UNIVERSITY**

GEOHERMAL TRAINING PROGRAMME
Orkustofnun, Grensásvegur 9,
IS-108 Reykjavík, Iceland

Reports 2013
Number 3

MODELLING AND STABILITY ANALYSIS OF BERLIN GEOHERMAL POWER PLANT IN EL SALVADOR

MSc thesis

School of Engineering and Natural Sciences
Faculty of Electrical and Computer Engineer
University of Iceland

by

Luis Alonso Aguirre Lopez

LaGeo S.A. de C.V.

15 Av. Sur, Colonia Utila

Santa Tecla, La Libertad

EL SALVADOR, C.A.

aguirrel@lageo.com.sv, luismvp1@gmail.com

United Nations University
Geothermal Training Programme
Reykjavík, Iceland
Published in November 2013

ISBN 978-9979-68-334-6

ISSN 1670-7427

This MSc thesis has also been published in April 2013 by the
School of Engineering and Natural Sciences
Faculty of Electrical and Computer Engineer
University of Iceland

INTRODUCTION

The Geothermal Training Programme of the United Nations University (UNU) has operated in Iceland since 1979 with six month annual courses for professionals from developing countries. The aim is to assist developing countries with significant geothermal potential to build up groups of specialists that cover most aspects of geothermal exploration and development. During 1979-2013, 554 scientists and engineers from 53 developing countries have completed the six month courses, or similar. They have come from Asia (39%), Africa (34%), Central America (15%), Central and Eastern Europe (11%), and Oceania (1%) There is a steady flow of requests from all over the world for the six month training and we can only meet a portion of the requests. Most of the trainees are awarded UNU Fellowships financed by the Government of Iceland.

Candidates for the six month specialized training must have at least a BSc degree and a minimum of one year practical experience in geothermal work in their home countries prior to the training. Many of our trainees have already completed their MSc or PhD degrees when they come to Iceland, but several excellent students who have only BSc degrees have made requests to come again to Iceland for a higher academic degree. From 1999 UNU Fellows have also been given the chance to continue their studies and study for MSc degrees in geothermal science or engineering in co-operation with the University of Iceland. An agreement to this effect was signed with the University of Iceland. The six month studies at the UNU Geothermal Training Programme form a part of the graduate programme.

It is a pleasure to introduce the 34th UNU Fellow to complete the MSc studies at the University of Iceland under the co-operation agreement. Luis Alonso Aguirre Lopez, BSc in Electrical Engineering from LaGeo S.A. de C.V. completed the six month specialized training in Geothermal Utilization at the UNU Geothermal Training Programme in October 2011. His research report was entitled: “Main considerations in the protection system design for a geothermal power plant”. After one year of geothermal research work in El Salvador, he came back to Iceland for MSc studies at the Faculty of Electrical and Computer Engineering in August 2011. In April 2013, he defended his MSc thesis presented here, entitled “Modelling and stability analysis of Berlin geothermal power plant in El Salvador”. His studies in Iceland were financed by the Government of Iceland through a UNU-GTP Fellowship from the UNU Geothermal Training Programme. We congratulate him on his achievements and wish him all the best for the future. We thank the Faculty of Electrical and Computer Engineering at the School of Engineering and Natural Sciences of the University of Iceland for the co-operation, and his supervisors for the dedication.

Finally, I would like to mention that Luis’ MSc thesis with the figures in colour is available for downloading on our website www.unugtp.is, under publications.

With warmest greetings from Iceland,

Ludvik S. Georgsson, director
United Nations University
Geothermal Training Programme

ACKNOWLEDGEMENTS

My sincere gratitude to the United Nation University Geothermal Training Programme (UNU-GTP) through its director Dr. Ingvar Fridleifsson (now retired) for supporting my master studies at the University of Iceland.

Special thanks to my supervisor Dr. Magni Þór Pálsson for his invaluable guidance, support and patience, as well for the encouragement which made this project possible.

I want to thanks also to staff of UNU-GTP: Mr. Lúdvík S. Georgsson, Ms. Thórhildur Ísberg, Mr. Ingimar G. Haraldsson, Ms. Málfrídur Ómarsdóttir and Mr. Markús A.G. Wilde for their patient, dedication and support throughout during this period.

My grateful thanks to my employer, LaGeo S.A. de C.V. in El Salvador for allowing me to do these studies with the UNU-GTP scholarship and supporting me during this period. My gratitude to the people that made this project possible with their invaluable support during the process: Mr. Rodolfo Herrera, Mr. Jorge Burgos, Mr. Ricardo Escobar and Mr. José Luis Henríquez.

My gratitude to C. Melgar, J.C. Pérez, F. Serrano, I. Perez, M. Avila. J.L. Henríquez, J. Estevez, J. Vazquez, C. Cuellar, J.C. Hamann for helping me with technical information and answering my questions.

Last but not least, I warmly thank my parents, Luis and Kenny, for they guidance and support through my life, my family and friends for their support and for taking care of my wife and daughter during this period and to the unconditional friend God, who makes all thinks possible.

DEDICATION

*To Maricela
for her love and unconditional support since 1999
and Mónica for making my life happier.*

ABSTRACT

Power system stability can be defined as the property of a power system that enables it to remain in a state of operating equilibrium under normal operating conditions and to regain an acceptable state of equilibrium after being subjected to a disturbance. There are different forms of power systems stability, but this project is focused on rotor angle stability.

Rotor angle stability is the ability of interconnected synchronous machines of a power system to remain in synchronism. For convenience in analysis and for gaining useful insight into the nature of stability problems, rotor angle stability phenomena are characterized in two categories:

- Small-signal stability: is the ability of the power system to maintain synchronism under small disturbances like variation in load and generation.
- Transient stability is the ability of the power system to maintain synchronism when subjected to a severe transient disturbance like short-circuits of different types.

Energy consumption in El Salvador has had an increase of 220.6% since 1995, caused by the industrial and commercial growing in the country and the increase in the population. The peak power demand in 1995 was 591.7 MW compared with peak power demand in 2011 of 962 MW. This power consumption increase required the construction of new power plants to satisfy the demand (SIGET, 2011).

Since 2007, Berlin Geothermal power plant has had an installed capacity increase of 46 MW with the installation of two new generators. There are also new plans about the installation of two more generators around 2015, with a total capacity of 35 MW. This growing will cause changes in power flow and dynamics characteristic of the power system that have to be taken into account for the development of geothermal energy in El Salvador.

A dynamic simulation model of Berlin geothermal power plant in El Salvador is built with Matlab/Simulink with the objective of doing a dynamic study of the system taking into account the future generators. This study let us to analyse the dynamic behaviour of the power plant with small and severe disturbances in the power system.

The dynamic study take into account the most important parts of the geothermal power plant like Turbine, Governor, Generator, Excitation system, transformers and transmission lines to get a good approximation of the systems and acceptable results.

TABLE OF CONTENTS

	Page
1. INTRODUCTION.....	1
2. THERMODYNAMICS CYCLES DESCRIPTION	2
2.1 Single flash.....	2
2.2 Organic rankine cycle.....	2
3. EL SALVADOR 115 KV ELECTRICAL SYSTEM	4
3.1 Transmission system interruptions	4
4. MAIN COMPONENTS DESCRIPTION	5
4.1 Turbine	5
4.1.1 Steam turbine	5
4.1.2 Straight condensing turbine.....	5
4.1.3 Gas turbine	5
4.2 Synchronous generator	6
4.3 Governor.....	8
4.4 Excitation system.....	9
4.5 Power transformer	10
4.6 Transmission lines.....	11
4.7 Power system stability	11
4.7.1 Power versus angle relationship.....	12
4.7.2 Rotor angle stability	12
4.7.3 Stability of dynamic systems.....	13
4.7.4 Eigenvalues and stability.....	15
4.7.5 Prony analysis	16
5. MODELLING DESCRIPTION	17
5.1 Simulink description.....	17
5.2 SimPowerSystems library	17
5.3 Excitation system modelling.	17
5.3.1 Limiters	17
5.3.2 Single time constant block with non-windup limiter.	18
5.3.3 Integrator block with non-windup limiter.	19
5.3.4 F_{EX} block	20
5.4 Governor modelling.....	21
5.5 Generating unit group modelling.....	22
5.6 CGB modelling.....	22
6. SIMULATION RESULTS.....	23
6.1 Base case simulation.....	23
6.1.1 Field voltage and stator voltage plots.....	23
6.1.2 Turbine-governor mechanical power	23
6.1.3 Rotor Speed.....	24
6.1.4 Load angle.....	25
6.1.5 Active and reactive power.....	25
6.2 Case 1 modelling	25
6.2.1 Rotor speed.....	26
6.2.2 Load angle.....	26
6.2.3 Stator voltage	27
6.2.4 Eigenvalues and eigenvectors.	27
6.2.5 Inherent stability.....	28
6.3 Case 2 modelling	29
6.3.1 Rotor speed.....	29

	Page
6.3.2 Load angle.....	30
6.3.3 Stator voltage	30
6.3.4 Eigenvalues and eigenvectors.	31
6.4 Case 3 modelling	32
6.4.1 Rotor speed.....	32
6.4.2 Load angle.....	32
6.4.3 Stator voltage	33
6.4.4 Eigenvalues and eigenvectors.	33
6.5 Case 4 modelling	34
6.5.1 Rotor speed.....	35
6.5.2 Load angle.....	35
6.5.3 Stator voltage	35
6.5.4 Eigenvalues and eigenvectors.	36
6.6 Case 5 modelling	37
6.6.1 Rotor speed.....	37
6.6.2 Load angle.....	38
6.6.3 Stator voltage	38
6.6.4 Eigenvalues and eigenvectors.	38
6.7 Case 6 modelling	39
6.7.1 Rotor speed.....	40
6.7.2 Load angle.....	40
6.7.3 Stator voltage	40
6.7.4 Eigenvalues and eigenvectors.	41
7. CONCLUSIONS.....	42
REFERENCES.....	44
APPENDIX A: Matlab code for base case plots	45
APPENDIX B: Typical Matlab code for case 1 to case 6 plots	47
APPENDIX C: Matlab code for eigenvectors plots and damping factor calculation	49
APPENDIX D: El Salvador electrical system single line diagram for 2015.....	52

LIST OF FIGURES

1. The single flash cycle.....	2
2. The ORC cycle.....	3
3. Electrical system in El Salvador (SIGET, 2011).....	4
4. Steam turbine rotor.....	5
5. Straight condensing turbine (IEEE,1985)	5
6. GE turboexpander (www.ge-energy.com)	5
7. Three-phase synchronous machine (Kundur, 1994)	6
8. Cross-sections of salient and cylindrical four pole machine (ONG, 1998).....	7
9. Speed governor and turbine in relationship to generator (Siemens, 2012)	8
10. TGOV1 Steam turbine-governor.....	9
11. General functional block diagram for synchronous machine excitation control system	9
12. Transfer functions for the Berlin power plant excitation systems.	10
13. PI section representation for transmission	11
14. Power-angle curve.....	12
15. Power-angle curves during a fault.....	13

	Page
16. Limiters representation.....	18
17. Transient response for a first-order transfer functions with windup and non-windup limiter	18
18. Single time constant block with non-windup limiter (IEEE, 1992).....	19
19. Single time constant block with non-windup limiter modelled in Simulink.....	19
20. Integrator block with non-windup limiter (IEEE, 1992).....	19
21. Integrator block with non-windup limiter modelled in Simulink.	20
22. F _{EX} block modelled in Simulink.....	20
23. AC1A excitation system modelled in Simulink.....	21
24. DESC-200 excitation system modelled in Simulink.....	21
25. TGOV1 turbine-governor modelling in Simulink.....	21
26. Generating unit group modelled in Simulink.....	22
27. CGB base case modelled in Simulink.....	23
28. Field voltage CGB base case	24
29. Stator voltage CGB base case	24
30. Turbine-governor mechanical power CGB base case.....	24
31. Rotor speed CGB base case	25
32. Load angle CGB base case.....	25
33. Active power CGB base case.....	25
34. Reactive power CGB base case.....	26
35. CGB Case 1 modelled in Simulink	26
36. Rotor Speed CGB case 1.....	27
37. Load Angle CGB case 1.....	27
38. Stator voltage CGB case 1	27
39. Stator voltage during fault occurrence for case 1.....	28
40. Eigenvectors case 1.....	28
41. Load angle differences case 1	29
42. CGB case 2 modelled in Simulink	29
43. Rotor speed CGB case 2	30
44. Load Angle CGB case 2.....	30
45. Stator voltage CGB case 2	30
46. Stator voltage during fault occurrence for case 2.....	31
47. Eigenvectors case 2.....	31
48. CGB case 3 modelled in Simulink	32
49. Rotor speed CGB case 3	32
50. Load angle CGB case 3.....	33
51. Stator voltage CGB case 3	33
52. Stator voltage during fault occurrence for case 3.....	33
53. Eigenvectors case 3.....	34
54. CGB case 4 modelled in Simulink	34
55. Rotor speed CGB case 4	35
56. Load angle CGB case 4.....	35
57. Stator voltage CGB case 4	35
58. Stator voltage during load increase for case 4	36
59. Eigenvectors case 4.....	36
60. CGB case 5 modelled in Simulink	37
61. Rotor speed CGB case 5	37
62. Load angle CGB case 5.....	38
63. Stator voltage CGB case 5	38
64. Stator voltage during fault occurrence for case 5.....	38
65. Eigenvectors case 5.....	39
66. CGB case 6 modelled in Simulink	39
67. Rotor speed CGB case 6	40
68. Load angle CGB case 6.....	40
69. Stator voltage CGB case 6	40
70. Stator voltage during fault occurrence for case 6.....	41

	Page
71. Eigenvectors case 6.....	41
72. Reactive power CGB case 1.....	43
73. Field voltage CGB case 1.....	43

LIST OF TABLES

1. Transmission system interruption distribution.....	4
2. Steam and gas turbines technical characteristic	6
3. Synchronous generators technical characteristic.....	7
4. Disturbances detail for CGB analysis	22
5. Eigenvalues, eigenvectors, frequency and damping ratio for case 1.....	28
6. Eigenvalues, eigenvectors, frequency and damping ratio for case 2.....	31
7. Eigenvalues, eigenvectors, frequency and damping ratio for case 3.....	34
8. Eigenvalues, eigenvectors, frequency and damping ratio for case 4.....	36
9. Eigenvalues, eigenvectors, frequency and damping ratio for case 5.....	39
10. Eigenvalues, eigenvectors, frequency and damping ratio for case 6.....	41

ABBREVIATIONS

15SEPT:	15 de Septiembre bus
BER:	Berlin bus
CGB:	Berlin geothermal power plant
DF:	Double flash cycle
ORC:	Organic Rankine cycle.
SF:	Single flash cycle
SC:	Short circuit
SM:	San Miguel bus

1. INTRODUCTION

Geothermal energy is one of the most important forms of renewable energy and it has several uses around the world. In 2009, electricity was produced from geothermal energy in 24 countries, increasing by 20% from 2004 to 2009 (Fridleifsson and Haraldsson, 2011). The countries with the highest geothermal installed capacity in MW were USA (3,093 MW), Philippines (1,197 MW), Indonesia (1,197 MW), Mexico (958 MW) and Italy (843 MW). In terms of the percentage of the total electricity production, the top five countries were Iceland (25%), El Salvador (25%), Kenya (17%), Philippines (17%) and Costa Rica (12%) (Bertani, 2010).

There are two geothermal fields in El Salvador that have operating power plants: Ahuachapán and Berlin. Their combined installed capacity is 204.4 MW.

Ahuachapán geothermal power plant consists of three units, two of them are condensing units, single flash cycle (SF) 30 MW each, and one condensing unit, double flash cycle (DF) of 35 MW. Berlin Geothermal power plant consists of four units, three of them, unit 1 and unit 2 of 28 MW each and unit 3 of 44 MW, are SF and the other one is an Organic Rankine cycle (ORC) of 9.2 MW (Guidos and Burgos, 2012).

Berlin Geothermal Power plant (CGB), the one object of study in this project, has as projections of new development, the construction of one condensing unit SF of 28 MW and one ORC of 9.2 MW as future projects. The new power generation developments at CGB cause changes in power flow and dynamics characteristic of the electrical system in El Salvador, but specially affects the dynamic behaviour of the existing units.

The purpose of this thesis is to make a detailed dynamic model of the power plant together with the surrounding power grid, to be able to perform the dynamic studies of the power plant, taking into account the existing and future units. The dynamic simulation model of CGB is performed with SymPowerSystems, a package of Matlab/Simulink, which is a design tool that allows the building models that simulate power systems.

For the model building, the following data were used: the database of the transmission line company in El Salvador (ETESAL, 2015), the database of the electrical market administrator in El Salvador (UT, 2013), and the manufacturer's data sheets and information given by the owner of CGB (LaGeo S.A. de C.V.).

2. THERMODYNAMICS CYCLES DESCRIPTION

Geothermal power plants can be divided into two main groups, steam cycles and binary cycles. Typically the steam cycles are used at higher well enthalpies, and binary cycles for lower enthalpies. The steam cycles allow the fluid to boil, and then the steam is separated from the brine and expanded in a turbine. Usually the brine is re-injected into the geothermal reservoir (SF) or it is flashed again at a lower pressure (DF).

A binary cycle uses a secondary working fluid in a closed power generation cycle. A heat exchanger is used to transfer heat from the geothermal fluid to the working fluid. Two typical binary cycles are the Organic Rankine Cycle (ORC) and the Kalina Cycle.

CGB only has two kinds of cycles: SF and ORC. Both of them are described below (Valdimarsson, 2011).

2.1 Single Flash

A flow sheet of the SF cycle is shown in Figure 1. The geothermal fluid enters the well at point 1. Because of the well pressure loss the fluid has started to boil at point 2, when it enters the separator. The brine from the separator is at point 3, and is re-injected at point 4. The steam from the separator is at point 5, where the steam enters the turbine. The steam is then expanded through the turbine down to point 6, where it is condensed in the condenser. The water in the condenser is re-injected at point 7.

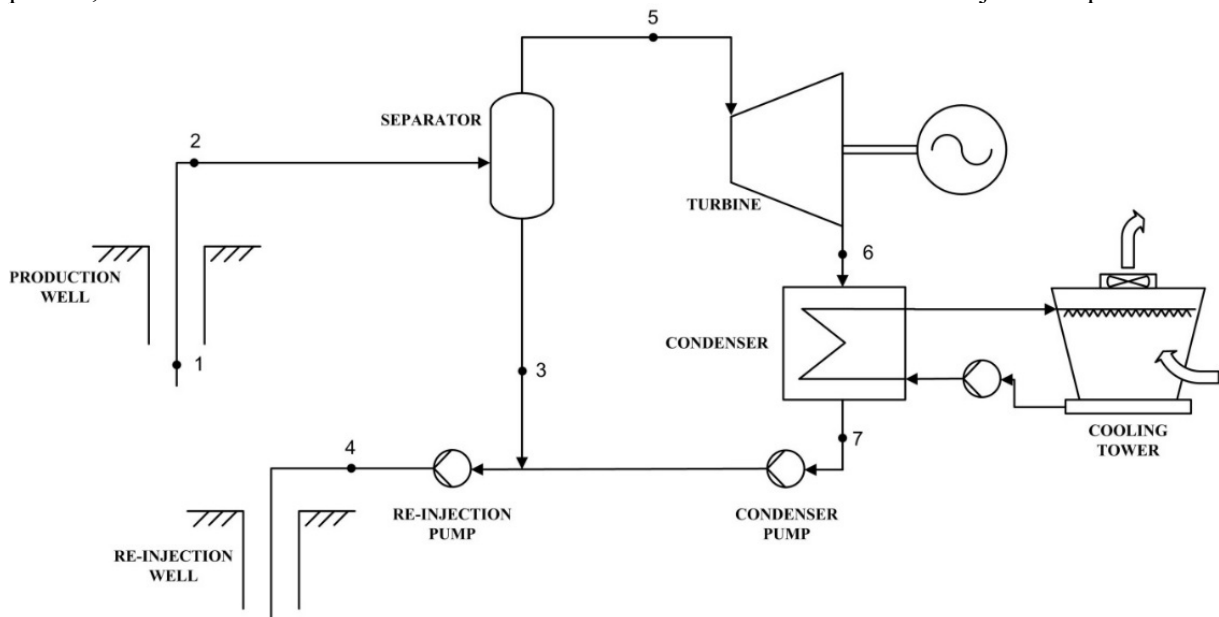


FIGURE 1: The Single flash cycle

2.2 Organic rankine cycle

ORC used two fluid in the process, geothermal fluid as process fluid and Isopentane as working fluid. A flow sheet of the ORC cycle is shown in Figure 2. The geothermal fluid enters the well at point 8. The fluid is then cooled down in the boiler and pre-heater, and sent to re-injection at point 10.

Pre-heated working fluid enters the preheater at point 3 and then the boiler at point 4. The fluid is heated to saturation in the boiler, or even superheated in some cases. The steam leaves the boiler at point 5 and enters the turbine.

The exit steam from the turbine enters the regenerator at point 6, where the heat in the steam can be used to pre-heat the condensed fluid prior to preheater inlet. The cooled steam enters the condenser at point 7 where is condensed down to saturated liquid at point 1.

A circulation pump raises the pressure from the condenser pressure to the high pressure level in point 2. There the fluid enters the regenerator for pre-heat before preheater entry.

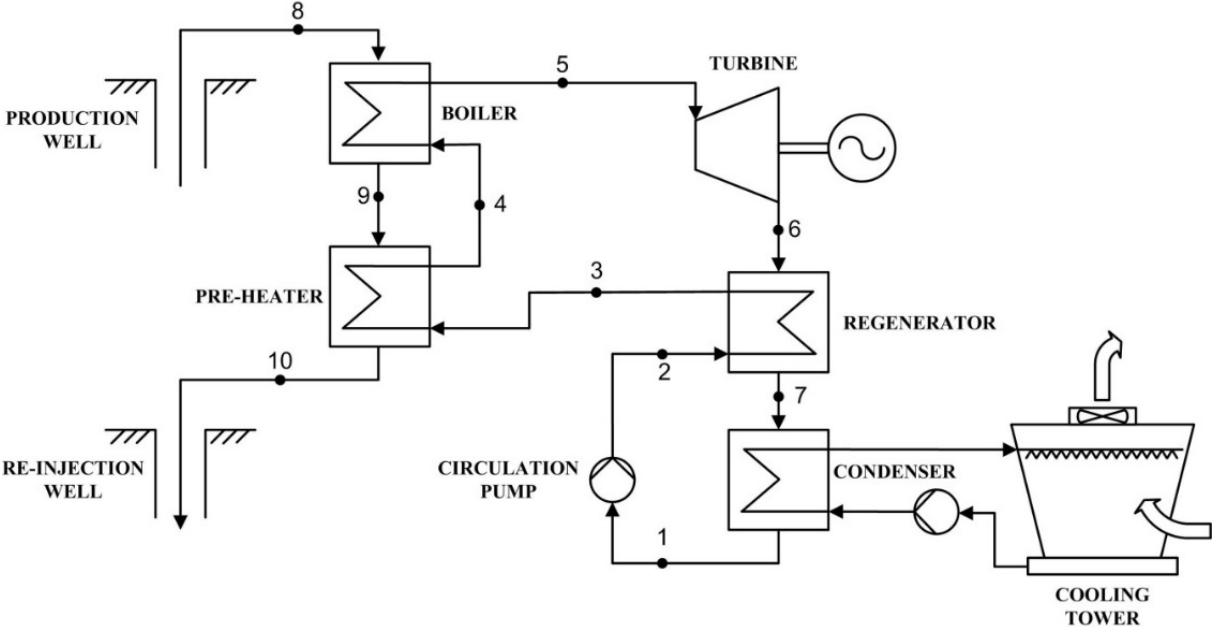


FIGURE 2: The ORC cycle

3. EL SALVADOR 115 KV ELECTRICAL SYSTEM

The generation distribution in the Salvadorian electrical system is composed of different kinds of power plants, like Hydroelectric (34.3%), Geothermal (24.5%), Fuel (36.3%) and Biomass (2%). The rest of energetic matrix is covered with imports. In 2011, the total installed capacity of electrical power in El Salvador was 1,477.2 MW, with an annual increase of 1.1%, respect to 2010 because of the start of operation for generators installed in Chaparrastique sugar mill, with a capacity of 16 MW (SIGET, 2011).

El Salvador covers an area of 21.000 km², and its national transmission system is composed of 38 lines of 115 kV, which have a total length of 1072.49 km. Otherwise, there are two lines of 230 KV that interconnect the transmission system of El Salvador with transmission system of Guatemala and Honduras. The length of the line to Guatemala is 14.6 km and 92.9 km to Honduras. There are 23 substations with a transformation capacity of 2,386.7 MVA. Figure 3 shows the one line diagram of the electrical system in El Salvador.



FIGURE 3: Electrical system in El Salvador (SIGET, 2011)

The maximum demand of the electrical system during 2011 was 962 MW, with an annual growth of 1.5% compared to 2010. There is a small amount of small hydroelectric generators connected directly to the distribution system at 46 KV with an installed capacity of 26.3 MW and an available capacity of 24.1 MW.

3.1 Transmission system interruptions

The number of interruptions registered during 2011, including the interconnections lines (230 KV) and the scheduled maintenances were 2,014 with an annual reduction of 2.4% compared to 2010. Form the total number of interruptions, the 55.01% was because of fails in the transmission systems and 29.5% for the maintenance of them. Table 1 shows a comparison of interruptions between 2010 and 2011.

TABLE 1: Transmission system interruption distribution

Interruption	2009	2010
Transmission line fail	65	71
Transmission line maintenance	147	144
Distribution line fail	1148	1108
Distribution line maintenance	610	594
Interconnection line fail (230 kV)	40	43
Interconnection line maintenance	35	32
Total	2045	1192

4. MAIN COMPONENTS DESCRIPTION

The goal of this project was the dynamic study of CGB and the analyses of the behaviour of each generator during perturbations in the electrical network. To perform this study all components involved in the stability analysis were modelled. These components are described below.

4.1 Turbine

There are two kinds of turbines at CGB, Steam turbines for unit 1, unit 2 and unit 3, that works with a SF cycle and gas turbines for unit 4 that works with ORC. Both kinds of turbines are described below.

4.1.1 Steam turbine

Steam turbines convert stored energy of high pressure and high temperature steam into rotating energy, which is in turn converted into electrical energy by the generator. The heat source for the boiler supplying the steam in this case is geothermal energy (Kundur, 1994).

Steam turbines consist of two or more turbine sections or cylinders coupled in series. Each turbine section has a set of moving blades attached to the rotor and a set of stationary vanes. The stationary vanes referred to as nozzle sections, form nozzles that accelerate the steam at high velocity. The kinetic energy of this high velocity steam is converted into shaft torque by the moving blades. Figure 4 shows a steam turbine rotor.



FIGURE 4: Steam turbine rotor

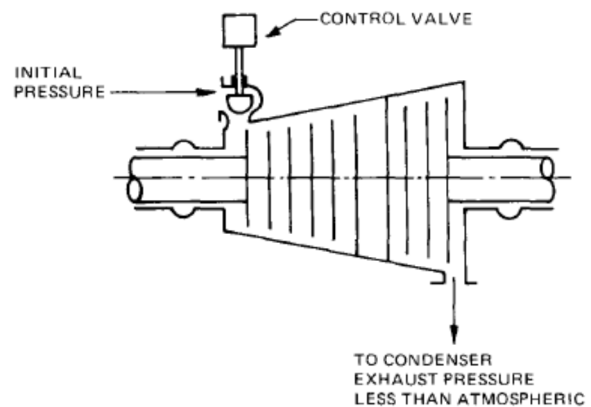


FIGURE 5: Straight condensing turbine (IEEE,1985)

4.1.2 Straight Condensing turbine

Steam turbines of CGB are type straight condensing, where all the steam enters the turbine at one pressure and all the steam leaves the turbine exhaust at a pressure below atmospheric pressure. (IEEE, 1985). Figure 5 shows a schematic diagram of a straight condensing turbine.

4.1.3 Gas turbine

Gas turbine for this particular case is a Turboexpander-generator group. A turboexpander expands process fluid from the inlet pressure to the discharge pressure in two steps; first through variable inlet guide vanes (or nozzles assembly) and then through the radial wheel. As the accelerated process fluid moves from the inlet guide vanes to the expander wheel, kinetic energy is converted into useful mechanical energy. The mechanical energy drives the generator.

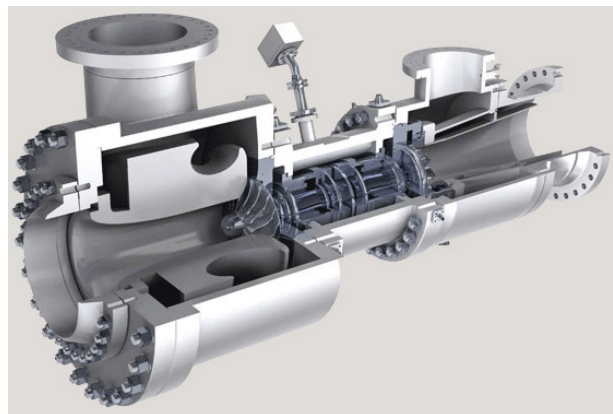


FIGURE 6: GE turboexpander (www.ge-energy.com)

The nozzles are controlled by an electrically governed hydraulic amplifier, acting upon the assembly through an actuator rod. The actuator turns a low level electrical signal from the Woodward governor to a rotary mechanical output, exerting an opening or a close force depending on the supplied oil pressure. Figure 6 shows a sectional diagram of a General Electric turbonexpander, similar to the one installed at Berlin.

Table 2 shows the technical characteristic of the steam and gas turbines that are part of the study of this document. The modelling of the turbine in Simulink will be shown altogether with governor in a later section.

TABLE 2: Steam and gas turbines technical characteristic

Interruption	Unit 1	Unit 2	Unit 3	Unit 4
Nominal power (MW)	28.12	28.12	44	9.2
Nominal speed (RPM)	3600	3600	3600	6500
Number of stages	9	9	7	1

4.2 Synchronous Generator

Synchronous generator consists of two essential elements: the field and the armature and the field winding is excited by direct current. When the rotor is driven by a turbine, the rotating magnetic field of the field winding induces alternating voltages in the three-phase armature winding of the stator. The frequency of the induced alternating voltages and of the resulting current that flow in the stator windings when a load is connected depends on the speed of the rotor. The frequency of the stator electrical variables is synchronized with the rotor mechanical speed: hence the designation Synchronous generator (Kundur, 1994). Figure 7 shows the schematic of the cross section of a three-phase synchronous machine.

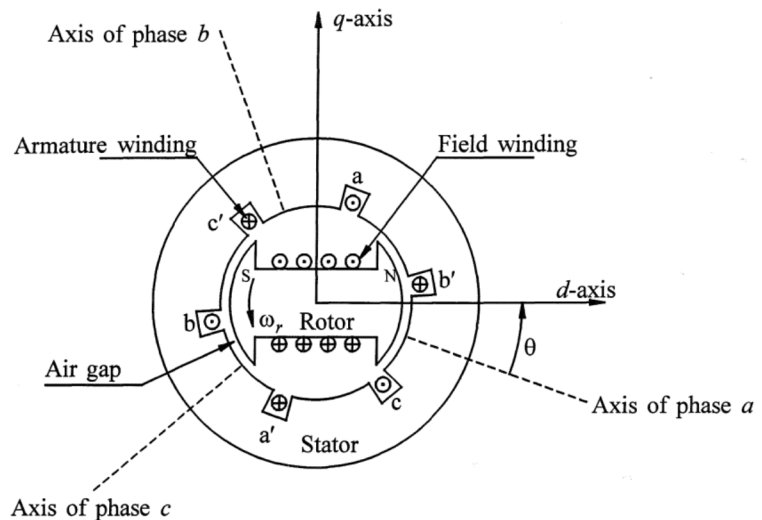


FIGURE 7: Three-phase synchronous machine (Kundur, 1994)

When two or more synchronous machines are interconnected, the stator voltages and currents of all the machines must have the same frequency and the rotor mechanical speed of each is synchronized to this frequency. Therefore, the rotors of all interconnected synchronous machines must be in synchronism.

Stator and rotor field reacts with each other and an electromagnetic torque results from the tendency of the two fields to align themselves. This electromagnetic torque opposes rotation of the rotor, so that mechanical torque must be applied by the prime mover to sustain rotation. The electrical torque output of the generator is changed only by changing the mechanical torque input by the turbine. An increase of mechanical torque input advance the rotor to a new position relative to the revolving magnetic field of the stator, a reduction of mechanical torque or power input will retard the rotor position. Under steady-state operating conditions, the rotor field and the revolving field of the stator have the same speed. However, there is an angular separation between them depending on the electrical torque output of the generator.

Armature winding operates at a considerably higher voltage than the field, because of that, armature require more space for insulation. Normal practice is to have the armature on the stator. The three-phase

windings of the armature are distributed 120° apart in space so that, with uniform rotation of the magnetic field, voltages displaced by 120° in time phase will be produced in the winding. Because the armature is subjected to a varying magnetic flux, the stator iron is built up of thin laminations to reduce eddy current losses.

The number of field poles is determined by the mechanical speed of the rotor and electrical frequency of stator currents. The synchronous speed is given by:

$$n = \frac{120f}{p_f} \quad (1)$$

where n is the speed in rev/min, f is the frequency in Hz and p_f is the number of field poles.

Depending on speed of the rotor, there are two basic structures used. Hydraulic turbines operate at low speed and therefore a relative large number of poles are required to produce the rated frequency. A rotor with salient or projecting poles and concentrated windings is more appropriate mechanically for this situation.

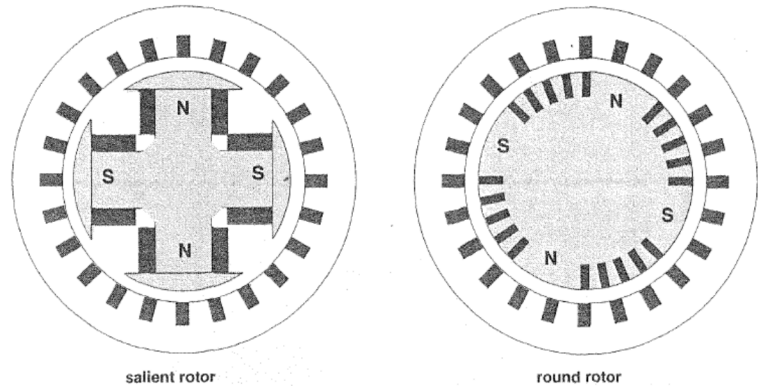


FIGURE 8: Cross-sections of salient and cylindrical four pole machine (ONG, 1998)

Steam and gas turbines, like our study case, on the other hand, operate at high speeds. Their generators have round or cylindrical rotors made up of solid steel forgings. They have two or four field poles, formed by distributed windings placed in slots milled in the solid rotor. Figure 8 shows the two types of rotors for synchronous generators.

With the purpose of identifying synchronous machine characteristics, two axes are defined as shown in Figure 4.4:

- The direct (d) axis, centred magnetically in the centre of the north pole.
- The quadrature (q) axis, 90 electrical degrees ahead of the d -axis.

The position of the rotor relative to the stator is measured by the angle θ between the d -axis and the magnetic axis of phase a winding.

Table 3 shows the technical characteristic of the synchronous generators part of the study of this project.

TABLE 3: Synchronous generators technical characteristic

Interruption	Unit 1	Unit 2	Unit 3	Unit 4
Nominal Voltage (kV)	13.8	13.8	13.8	13.8
Nominal power (MVA)	37	37	51.76	12.5
Active power (MW)	31.5	31.5	44	10
Power factor	0.85	0.85	0.85	0.8
Nominal frequency (Hz)	60	60	60	60
Inertia constant (MW-s/MVA)	2.4	2.4	1.36	3.71
Nominal speed (RPM)	3600	3600	3600	1800
Poles number	2	2	2	4

The modelling of the generator in Simulink has been done with the block *Synchronous machine pu Standard* of SimPowerSystem library that represent electrical part of the synchronous generator by a

sixth-order state space model and the mechanical part by the equations of motion described by Kundur (1994) and showed below:

$$\frac{d\Delta\bar{\omega}_r}{dt} = \frac{1}{2H} (\bar{T}_m - \bar{T}_e - K_D\Delta\bar{\omega}_r) \quad (2)$$

$$\frac{d\delta}{dt} = \omega_0\Delta\bar{\omega}_r \quad (3)$$

The model takes into account the dynamics of the stator, field and damper windings. The block requires the main parameters of the generator, like nominal power, line to line voltage, frequency, reactances, time constants and inertia. It is possible to simulate the saturation curve of the generator too, by field current and terminal voltage pairs. The more amounts of pairs, more accurate will be the model.

The block includes an output that is a vector containing 22 signals of the generator, they can be demultiplex by the Bus Selector Block provided in the Simulink library.

4.3 Governor

The prime mover governor systems provide a means of controlling power and frequency, a function commonly referred to as load-frequency control. Its basic function is to control speed and/or load. The governor receives speed signal input and controls the inlet valve/gate in steam turbines and the nozzles assembly for gas turbines, to regulate the power and frequency. The governing systems have three basic functions: normal speed/load control, overspeed control and overspeed trip. Additionally, the turbine controls include a number of other functions like start-up/shutdown controls and auxiliary pressure control. Prime mover governor consist of two main components:

- Turbine controls, that receive all field control signals from the turbine-generator group and generate a control command. Turbine controls can be mechanical-hydraulic, electrohydraulic or digital electrohydraulic.
- Actuator, that receives the control command from the turbine control and executes a control action over the inlet valve/gate in steam turbines and the nozzles assembly for gas turbines. Actuators are normally hydraulic.

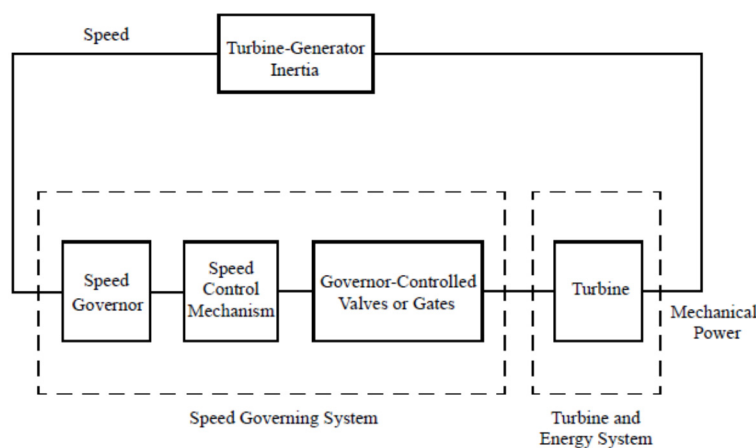


FIGURE 9: Speed governor and turbine in relationship to the generator (Siemens, 2012)

Figure 9 shows a turbine and governor functional diagram and its relationship with the generator.

The turbine-governor modelling in Simulink has been done by the transfer function of the TGOV1 Steam turbine governor, defined by PSSE governor blocks. Figure 10 shows the transfer function. This model represents governor action and the reheater time constant effect for a steam turbine. The ratio T_2/T_3 , equals the fraction of turbine power that is developed by the high-pressure turbine. T_3 is the reheater time constant and T_1 is the governor time constant (SIEMENS, 2012).

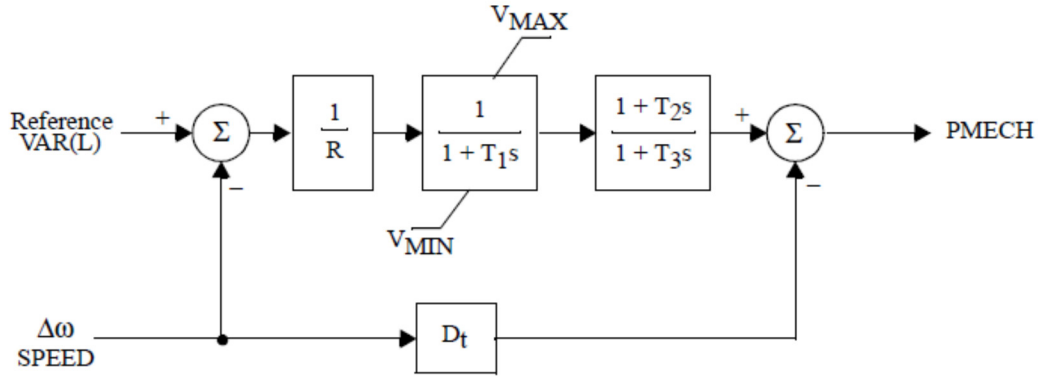


FIGURE 10: TGOV1 steam turbine-governor

4.4 Excitation system

Excitation system provides direct current to the synchronous machine field winding. Additionally, the excitation system performs control and protective functions that are essential to the satisfactory performance of the power system by controlling the field voltage and thereby the field current.

The control functions include control of voltage and reactive power flow, and the enhancement of system stability. The protective functions ensure that the capability limits of the synchronous machine, excitation system and other equipment are not exceeded.

The general functional block diagram shown in Figure 11 indicates various synchronous machine excitation subsystems. These subsystems may include a terminal voltage transducer and load compensator, excitation control elements, an exciter, and, in some cases (but not our study case), a power system stabilizer (IEEE 1992).

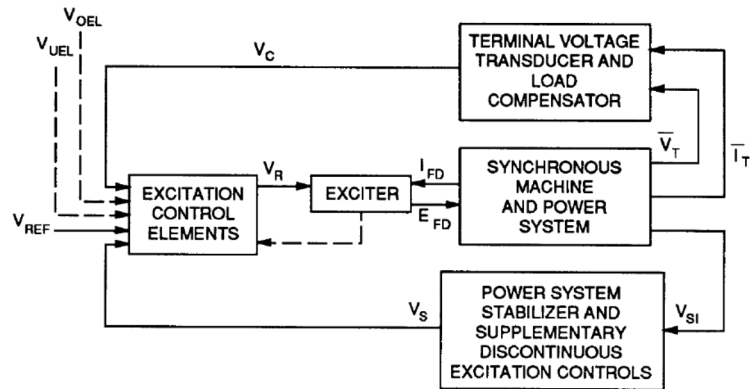


FIGURE 11: General functional block diagram for synchronous machine excitation control system (IEEE, 1992)

According to (IEEE 1992), three distinctive types of excitation systems are identified on the basis of excitation power source:

- Type DC excitation systems, which utilize a direct current generator with a commutator as the source of excitation system power.
- Type AC excitation systems, which use an alternator and either stationary or rotating rectifiers to produce the direct current needed for the synchronous machine field.
- Type ST excitation systems, in which excitation power is supplied through transformers or auxiliary generator windings and rectifiers.

The excitation system modelling in Simulink has been done by the transfer function of each particular model. Unit 1, Unit 2 and Unit 3 have an excitation system model AC1A, according to (IEEE, 1992). Unit 4 have a Basler Electric excitation system model DECS-200, which is not defined on (IEEE, 1992) but is expected to be part of the next revision of the standard. Figures 12 shows the transfer functions of both excitation systems.

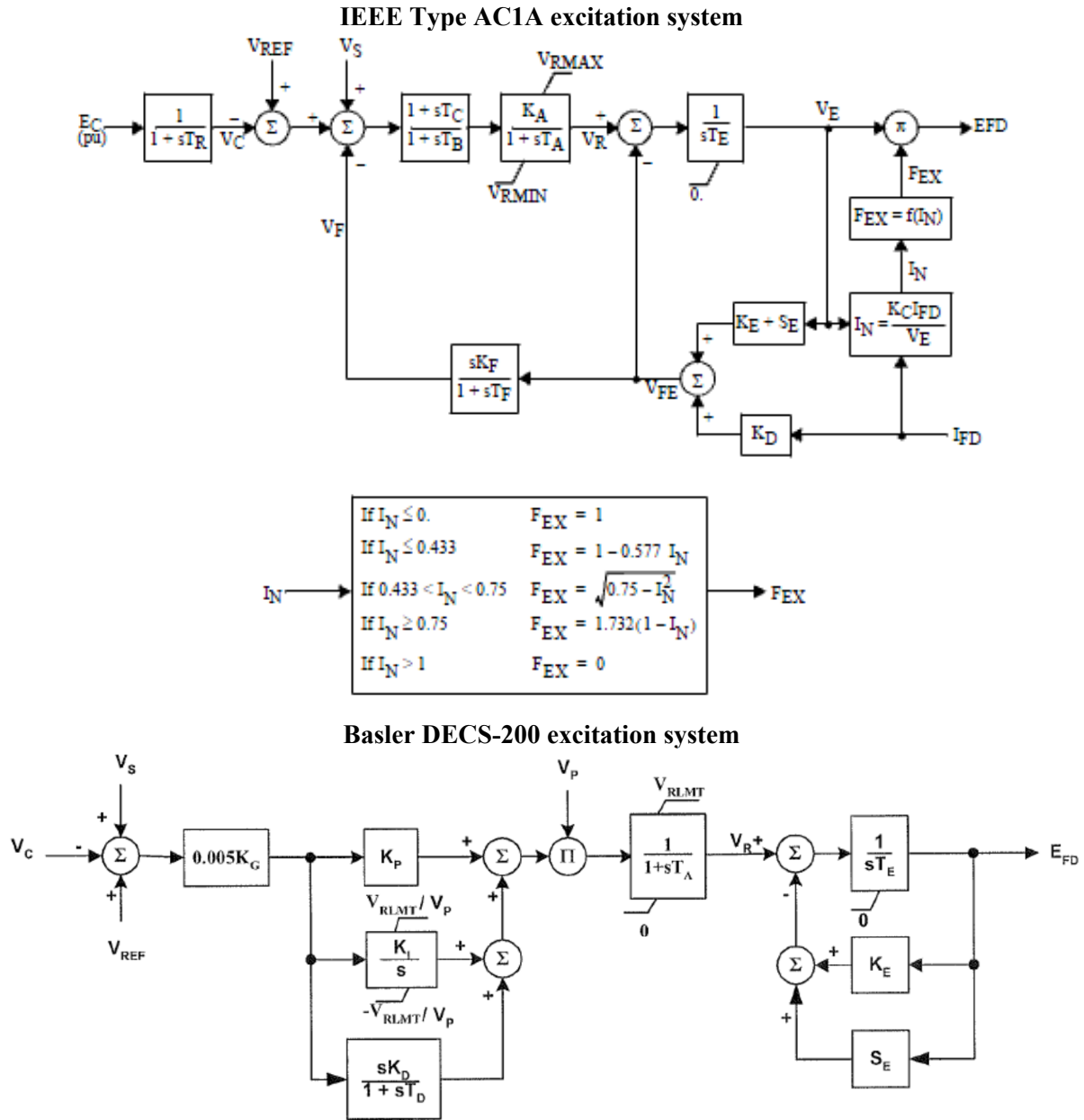


FIGURE 12: Transfer functions of the Berlin power plant excitation system

4.5 Power transformer

Power transformer is connected between the generator terminals and the transmission system and converts the voltage level of the generator to the transmission voltage level. Transformers in general, enable the utilization of different voltage levels across the system. From the viewpoint of efficiency and power-transfer capability, the transmission voltages have to be high to avoid losses.

The modelling of the transformer in Simulink has been done with the block *Three-phase Transformer (Two Windings)* of SimPowerSystem library that implements a three-phase transformer using three single-phase transformers. It is possible to simulate the saturation of the core, hysteresis and initial fluxes of the transformer. The simulation of these parameters can be unabled or disabled in the dialog box. Connection types of both winding of the transformer can be defined in the dialog box too.

Others parameters defined in the dialog box of the block are nominal power and frequency, voltage, resistance and inductance of both windings, magnetization resistance and reactance, saturation characteristic and initial fluxes (if they was unabled to be simulated).

4.6 Transmission lines

Electrical power is transferred from generating stations to consumers through overhead lines, which are used for long distances in open country in the power transmission system. A transmission line is characterized by four parameters: series resistance R due to the conductor resistivity, shunt conductance G due to leakage currents between the phases and ground, series inductance L due to magnetic field surrounding the conductors, and shunt capacitance C due to the electric field between conductors. Shunt conductance represents losses due to leakage currents along insulators strings and corona. In power lines, its effect is small and usually neglected (Kundur, 1994).

The modelling of the transmission lines in Simulink has been done with the block *Three-phase PI Section Line* of SimPowerSystem library that implements a three-phase transmission line model with parameters lumped in a PI section as shown in Figure 13. The line parameters R , L and C are specified as positive and zero sequence parameters that take into account the inductive and capacitive coupling between the three-phase conductors as well as the ground parameters. This method of specifying line parameters assumes that the three-phases are balanced. Using a single PI section model is appropriate for modelling short lines, which are defined as lines shorter than around 80 km (Kundur, 1994).

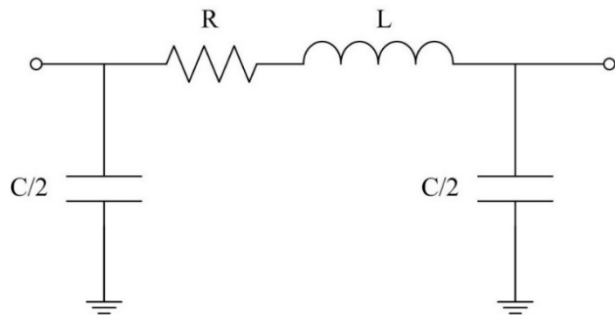


FIGURE 13: PI section representation for transmission

4.7 Power system stability

Power system stability is the ability of an electric power system, for a given initial operation condition, to regain a state of operating equilibrium after being subjected to a physical disturbance, with most system variables bounded so that practically the entire system remains intact. Theory of section 4.7 has been taken from Kundur et al. (2003) and Kundur (1994).

Previous definition applies to an interconnected power system as a whole. Often, however, the stability of a particular generator or group of generators is also of interest. A remote generator may lose stability (synchronism) without cascading instability of the main system.

Power systems are subjected to a wide range of small and large disturbances. Small disturbances in the form of load changes occur continually; the system must be able to adjust to the changing condition and operate satisfactorily. It must be also be able to survive numerous disturbances of a severe nature, such as a short circuit on a transmission line or loss of a large generator.

The response of the power system to a disturbance involves much of the equipment. For example, a fault on a critical element followed by its isolation by a protective relay will cause variations in power flows, network bus voltages and machine rotor speeds; the voltage variations will actuate both generators and transmission network voltage regulators; the generator speed variations will actuate prime movers governors and the voltage and frequency variations will affect the system loads to varying degrees depending on their individual characteristics. Besides, devices used to protect individual equipment may respond to variations in system variables and cause tripping of the equipment, thereby weakening the system and possibly leading to system instability.

If following a disturbance the power system is stable, it will reach a new equilibrium state with the system integrity preserved i.e., with practically all generators and loads connected through a single contiguous transmission system. Power systems are continually experiencing fluctuations of small magnitudes. However, for assessing stability when subjected to a specific disturbance, it is usually valid to assume that the system is initially in a true steady-state operating condition.

4.7.1 Power versus angle relationship

The relationship between interchange power and angular position of the rotors of synchronous machines is an important characteristic that has a bearing on power system stability. This relationship is nonlinear. To illustrate this we will consider a synchronous generator connected to a motor by a transmission line having an inductive reactance X_L .

The power transferred from the generator to the motor is a function of angular separation (δ) between the rotors of the two machines. This angular separation is due to three components: generator internal angle, angular difference between the terminal voltage of the generator and motor (caused by transmission line impedance) and internal angle of the motor. The power transferred from the generator to the motor is given by:

$$P = \frac{E_G E_M}{X_T} \sin \delta \quad (4)$$

Where subscript G and M refers to generator and motor respectively and $X_T = X_G + X_L + X_M$. The corresponding power versus angle relationship is plotted in Figure 14. As the angle is increased, the power transfer increases up to a maximum. After a certain angle, nominally 90° , a further increase in angle results in a decrease in power transferred. Angular separation (δ) for a particular generator is normally referred as rotor angle or load angle.

4.7.2 Rotor angle stability

Rotor angle stability is the ability of synchronous machines of an interconnected power system to remain in synchronism after being subjected to a disturbance. It depends on the ability to maintain/restore equilibrium between electromagnetic torque and mechanical torque of each synchronous machine in the system. Instability that may result occurs in the form of increasing angular swings of some generators leading to their loss of synchronism with other generators.

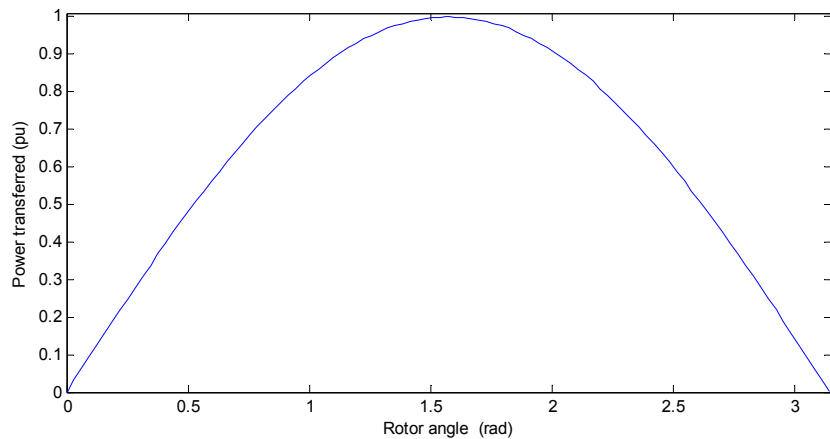


FIGURE 14: Power-angle curve

A rotor angle stability problem involves the study of the electromechanical oscillations inherent in power systems. A fundamental factor in this problem is the manner in which the power output of synchronous machines varies as their rotor angle change. Under steady state conditions, there is equilibrium between the input mechanical torque and the output electromagnetic torque of each generator, and the speed remains constant. If the system is perturbed, this equilibrium is upset, resulting in acceleration or deceleration of the rotors of the machines according to the laws of motion of a rotating body. If one generator temporarily runs faster than another, the angular position of its rotor relative to that of the slower machine will advance. The resulting angular difference transfers part of the load from the slow machine to the fast machine, depending on the power-angle relationship. This tends to reduce the speed difference and hence the angular separation.

The change in electromagnetic torque of a synchronous machine following a perturbation can be resolved into two components:

- Synchronizing torque component, in phase with rotor angle deviation.
- Damping torque component, in phase with the speed deviation.

System stability depends on the existence of both components of torque for each of the synchronous generators. Lack of synchronizing torque results in aperiodic or nonoscillatory instability, lack of damping torque results in oscillatory instability. For convenience in analysis, it is useful to characterize rotor angle stability in terms of the following two subcategories:

- Small Disturbance (or small signal) rotor angle stability, is concerned with the ability of the power system to maintain synchronism under small disturbances. The disturbances are considered to be sufficiently small that linearization of system equations is permissible for purposes of analysis. Small-disturbance stability depends on the initial operating state of the system. Instability that may result can be of two forms: increase in rotor angle through a non-oscillatory or aperiodic mode due to lack of synchronizing torque or rotor oscillations of increasing amplitude due to lack of sufficient damping torque.
- Large disturbance rotor angle stability or transient stability, as it is commonly referred to, is concerned with the ability of the power system to maintain synchronism when subjected to a severe disturbance, such as a short circuit on a transmission line. The resulting system response involves large excursions of generator rotor angles and is influenced by the nonlinear power-angle relationship. Transient stability depends on both the initial operating state of the system and the severity of the disturbance. Instability is usually in the form of aperiodic angular separation due to insufficient synchronizing torque, manifesting as first swing instability.

Small signal stability and transient stability are categorized as short term phenomena, with a time frame of interest on the order of 10-20 seconds following a disturbance. During transient stability phenomena, there are changes in the operation point of the power-angle relationship curve because of changes in reactance caused by loss of transmission lines or generators. Figure 15 shows typical power-angle relationship plot for the three network conditions; pre-fault, post-fault and during the fault.

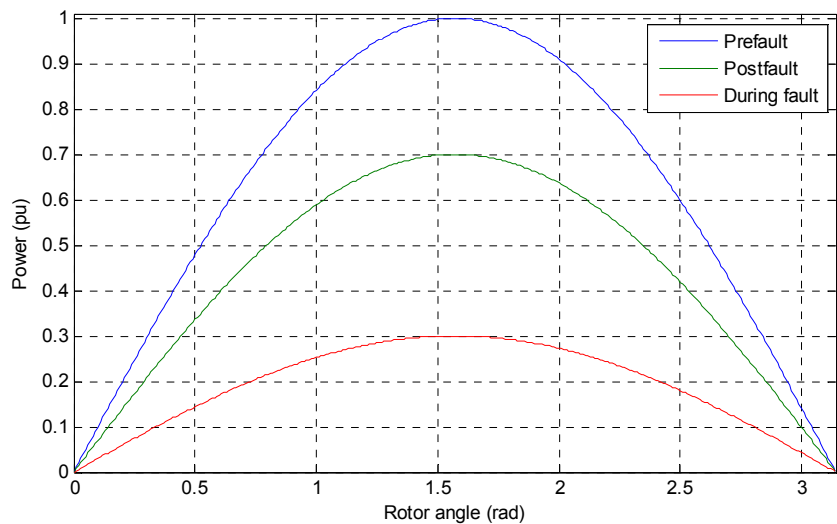


FIGURE 15: Power-angle curves during a fault

4.7.3 Stability of dynamic systems

Behaviour of dynamics systems, as a power system, can be described by a set of nonlinear ordinary differential equations of the following form:

$$\dot{x}_i = f_i(x_1, x_2, \dots, x_n; u_1, u_2, \dots, u_r; t) \quad i = 1, 2, \dots, n \quad (5)$$

Where n is the order of the system and r is the number of inputs. Equation 5 can be written in form of a vector-matrix notation:

$$\dot{x} = f(x, u, t) \quad (6)$$

Vector \mathbf{x} is the state vector, and its entries are the state variables. Vector \mathbf{u} is the vector of inputs to the system. These are the external signals that influence the performance of the system. The outputs variables can be observed on the system and may be expressed in terms of the state variables and the input variables in the following form:

$$\mathbf{y} = \mathbf{g}(\mathbf{x}, \mathbf{u}) \quad (7)$$

Where \mathbf{y} is the vector of outputs and \mathbf{g} is a vector of nonlinear functions relating state and inputs variables to output variables.

Any set of n linearly independent system variables can be used to describe the state of the system, referred as the state variables, and form a set of dynamics variables that, along with the inputs of the system, provide a complete description of the system behaviour. The state variables may be physical quantities as angle, speed, voltage or abstract mathematics variables associated with the differential equations that describe the dynamics of the system.

A system is locally stable about an equilibrium point if, when subjected to small perturbation, it remains within a small region surrounding the equilibrium point. Local stability conditions can be studied by linearizing the nonlinear system equations about the equilibrium point. An equilibrium point is where all derivatives of a differential equation are zero.

Let \mathbf{x}_0 be the initial state vector and \mathbf{u}_0 the input vector corresponding to the equilibrium point about which the small signal performance is to be investigated. Equation 6 can be rewritten as

$$\dot{\mathbf{x}}_0 = \mathbf{f}(\mathbf{x}_0, \mathbf{u}_0) = 0 \quad (8)$$

Assuming a small perturbation, Δx and Δu , Equation 8 can be expressed in terms of Taylor's series expansion. With terms involving second and higher order powers of Δx and Δu neglected, we can write:

$$\Delta \dot{x}_i = \frac{\partial f_i}{\partial x_1} \Delta x_1 + \dots + \frac{\partial f_i}{\partial x_n} \Delta x_n + \frac{\partial f_i}{\partial u_1} \Delta u_1 + \dots + \frac{\partial f_i}{\partial u_r} \Delta u_r \quad (9)$$

With $i=1, 2, \dots, n$. In a like manner, linearizing Equation 7, we get

$$\Delta y_j = \frac{\partial g_j}{\partial x_1} \Delta x_1 + \dots + \frac{\partial g_j}{\partial x_n} \Delta x_n + \frac{\partial g_j}{\partial u_1} \Delta u_1 + \dots + \frac{\partial g_j}{\partial u_r} \Delta u_r \quad (10)$$

With $j=1, 2, \dots, m$, the linearized form of Equations 6 and 7 are

$$\Delta \dot{\mathbf{x}} = \mathbf{A} \Delta \mathbf{x} + \mathbf{B} \Delta \mathbf{u} \quad (11)$$

$$\Delta \mathbf{y} = \mathbf{C} \Delta \mathbf{x} + \mathbf{D} \Delta \mathbf{u} \quad (12)$$

where

$$\mathbf{A} = \begin{bmatrix} \frac{\partial f_1}{\partial x_1} & \dots & \frac{\partial f_1}{\partial x_n} \\ \dots & \dots & \dots \\ \frac{\partial f_n}{\partial x_1} & \dots & \frac{\partial f_n}{\partial x_n} \end{bmatrix} \quad \mathbf{B} = \begin{bmatrix} \frac{\partial f_1}{\partial u_1} & \dots & \frac{\partial f_1}{\partial u_r} \\ \dots & \dots & \dots \\ \frac{\partial f_n}{\partial u_1} & \dots & \frac{\partial f_n}{\partial u_r} \end{bmatrix}$$

$$\mathbf{C} = \begin{bmatrix} \frac{\partial g_1}{\partial x_1} & \dots & \frac{\partial g_1}{\partial x_n} \\ \dots & \dots & \dots \\ \frac{\partial g_m}{\partial x_1} & \dots & \frac{\partial g_m}{\partial x_n} \end{bmatrix} \quad \mathbf{D} = \begin{bmatrix} \frac{\partial g_1}{\partial u_1} & \dots & \frac{\partial g_1}{\partial u_r} \\ \dots & \dots & \dots \\ \frac{\partial g_m}{\partial u_1} & \dots & \frac{\partial g_m}{\partial u_r} \end{bmatrix}$$

The partial derivatives are evaluated at the equilibrium point about which the small perturbation is being analysed. In Equations 11 and 12

- $\Delta \mathbf{x}$ is the state vector of dimension n
- $\Delta \mathbf{y}$ is the output vector of dimension m
- $\Delta \mathbf{u}$ is the input vector of dimension r
- \mathbf{A} is the state or plant matrix of size $n \times n$
- \mathbf{B} is the control or input matrix of size $n \times r$
- \mathbf{C} is the output matrix of size $m \times n$
- \mathbf{D} is the matrix which defines the proportion of input which appears directly in the output, size $n \times r$

4.7.4 Eigenvalues and stability

For power system stability studies, the characteristic of a system can be determined by the analysis of the eigenvalues of the linearized system. The eigenvalues of a matrix are given by the values of the scalar parameter λ for which there exist non-trivial solutions (i.e., other than $\phi=0$) to the equation

$$A\phi = \lambda\phi \quad (13)$$

where

A is the state $n \times n$ matrix (real for a physical system such as a power system)

ϕ is a $n \times 1$ vector

To find the eigenvalues, Equation 13 may be written in the form

$$(A - \lambda I)\phi = 0 \quad (14)$$

For a non-trivial solution

$$\det(A - \lambda I) = 0 \quad (15)$$

Expansion of the determinant gives the characteristic equation. The n solutions of $\lambda = \lambda_1, \lambda_2, \dots, \lambda_n$ are the eigenvalues of A . The eigenvalues may be real or complex. If A is real, complex eigenvalues always occur in conjugate pairs (Kundur, 1994).

The time dependent characteristic of a mode corresponding to an eigenvalue λ_i is given by $e^{\lambda_i t}$. A real eigenvalue correspond to a non-oscillatory mode. A negative real eigenvalue represent a decaying mode. A positive real eigenvalue represents aperiodic instability. Complex eigenvalues occur in conjugate pairs, and each pair corresponds to an oscillatory mode. Thus for a complex pair of eigenvalues:

$$\lambda = \sigma \pm j\omega \quad (16)$$

The real component of the eigenvalues gives the damping and the imaginary component gives the frequency of oscillation. A negative real part represents a damped oscillation (stable system) whereas a positive real part represents oscillation of increasing amplitude (unstable system). The frequency of oscillation is given by:

$$f = \frac{\omega}{2\pi} \quad (17)$$

This represents the actual or damped frequency. The damping ratio determines the rate of decay of the amplitude of the oscillation and is given by:

$$\zeta = \frac{-\sigma}{\sqrt{\sigma^2 + \omega^2}} \quad (18)$$

The damping ratio ζ determines the rate of decay of the amplitude of the oscillation; it means that amplitude decays to 37% of initial amplitude in $1/|\sigma|$ seconds or in $1/2\pi\zeta$ cycles of oscillation.

4.7.5 Prony analysis

Eigenvalue calculation is very complex for a power system that has non-linear components and where not all the information to develop the linearization is available. This is the case on the analysis object of the present project. In this case, Prony analysis is used for eigenvalues calculation.

Prony analysis estimate directly the frequency, damping, strength and relative phase of modal components presents in a given signal. Prony methods and their recent extensions are designed to directly estimate the eigenvalues λ_i (and eigenvectors) of a dynamic system by fitting a sum of complex damped sinusoids to evenly space sample (in time) values of the output described below (Hauer, Demeure, Scharf, 1990)

$$\hat{y}(t) = \sum_{i=1}^Q A_i e^{\sigma_i t} \cos(2\pi f_i t + \phi_i) \quad (19)$$

where

A_i is the amplitude of component i ,

σ_i is the damping coefficient of component i (real part of eigenvalues)

ϕ_i is the phase of component i

f_i is the frequency of component i (imaginary part of eigenvalues, $\omega_i = 2\pi f_i$)

Q : Total number of damped exponential components

For the Prony analysis in Matlab, there have been used Prony Toolbox (Singh, 2003), which is a software tool built around Matlab functions with a user-friendly graphical interface and containing all the necessary features to perform Prony Analysis.

With Prony Toolbox, it is possible to calculate the Eigenvalues and the poles of the system. Poles gives the angle of the eigenvector of the system, so it is possible to plot the eigenvector in a polar way, with amplitude A_i and angle ϕ_i for each generator group. Rotor speed signal have been used to perform Prony analysis.

Eigenvalues method for stability analysis can be applied just for small signal stability cases, where local stability conditions permits the linearization of the system. For the implementation of this method in cases with transient stability perturbations, like SC, the analysis is done during the time period that correspond to small signal stability conditions, avoiding the first cycles of the oscillation, that are part of transient stability phenomena.

5. MODELLING DESCRIPTION

Modelling of CGB required all the information and parameters of the components that are part of the system. Sometimes it is complicated to get these parameters and it is necessary to select typical values suggested by standard and references. The present model uses real parameters of the equipment nowadays installed and operating in the power plant, but in some particular cases because of lack of information or wrong data, a few parameters have been taken from typical values detailed by international standards. The detail of the modelling of each component will be described below.

5.1 Simulink description

Simulink is a software package that enables the users to model, simulate and analyse systems whose output change over time. Such systems are often referred to as dynamic systems. The Simulink software can be used to explore the behaviour of a wide range of real-world dynamic systems, including electrical, mechanical and thermodynamics systems.

Simulating a dynamic system is a two steps process. First, the user creates a block diagram, using the Simulink model editor, which graphically depicts time-dependent mathematical relationships among the system's inputs, states and outputs. The user then commands the Simulink software to simulate the system represented by the model from a specified start time to a specific stop time (Simulink, 2010).

Simulink provide a graphical editor that allows the user to create and connect instances of block types selected from library browser. Block types available include transfer functions block, integrators, constant, gain, math operators, signal routing, sinks, sources and others types of blocks from more specialized libraries like SimPowerSystems, that is the base of the modelling object of this project.

5.2 SimPowerSystems library

SimPowerSystem was designed to provide a modern design tool that allow rapidly and easily built models that simulate power systems. The libraries contain models of typical power equipment such as transformers, lines, machines and power electronics (Simulink, 2002).

The equipment that has been simulated using SimPowerSystems library blocks are: Generator, Transformer, transmission lines, circuit breakers, infinite bus, loads and three-phase faults. The equipment that has been simulated using Simulink by the transfer function modelling are: excitation system, governor and turbine. SimPowerSystems include in its libraries models for all this components, but any of them is the same type of the ones installed in CGB.

5.3 Excitation system modelling.

Excitation systems have been modelling through the transfer functions in Simulink. Figure 12 showed both excitation systems transfer function modelled in this project. Excitation system basically has been modelled by simple transfer functions, integrators and math operation blocks, but there are three particular blocks that required special attention during modelling; Single time constant block with non-windup limiter ($K_A/1+sT_A$) and F_{EX} block for AC1A exciter and Integrator block with non-windup limiter (K_I/s) for DECS-200 exciter.

5.3.1 Limiters

In excitation systems modelling, there are two types of limiters, windup and non-windup. In general terms, a limiter limits the output of a block within upper and lower values. These limits are encountered with integrators blocks and single time constant blocks in our case of study. The main difference between windup and non-windup limiters is the way in which the limited variable comes off its limits.

To illustrate that, we will use the transfer function in Figure 16, which shows both kind of limits representation. The time domain simulation of the output $x(t)$ for both cases, for a pulse input excitation $u(t)$ of 1V, is shown in Figure 17.

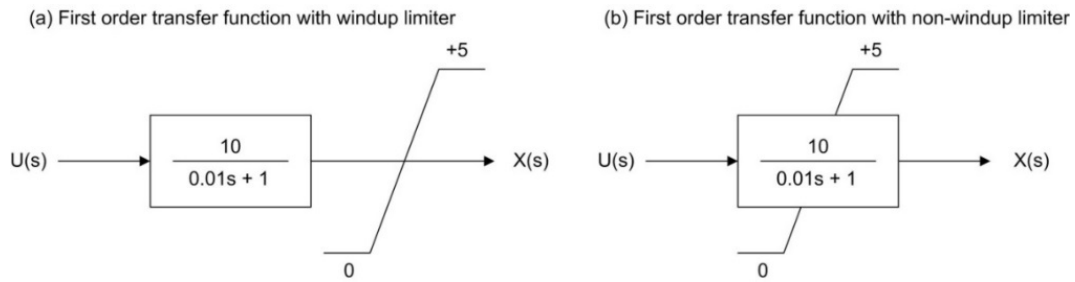


FIGURE 16: Limiters representation

The output variable $x(t)$ reaches its limit at the same time for both cases, but $x(t)$ backs off the limit first for the non-windup limiter. The reason is that for the windup limiter the output variable is just clipped at the limit, whereas in the non-windup limiter the differential equation is actually modified (Bonatto and Dommel, 2002).

Simulink has in its library a saturation block that works as a windup limits, but the non-windup limit is not available in the library, because of that it was necessary to create it, as it will be described here. We will start with the amplifier block (single time constant block) because it was the first one to be created using Bonatto and Dommel (2002) as references.

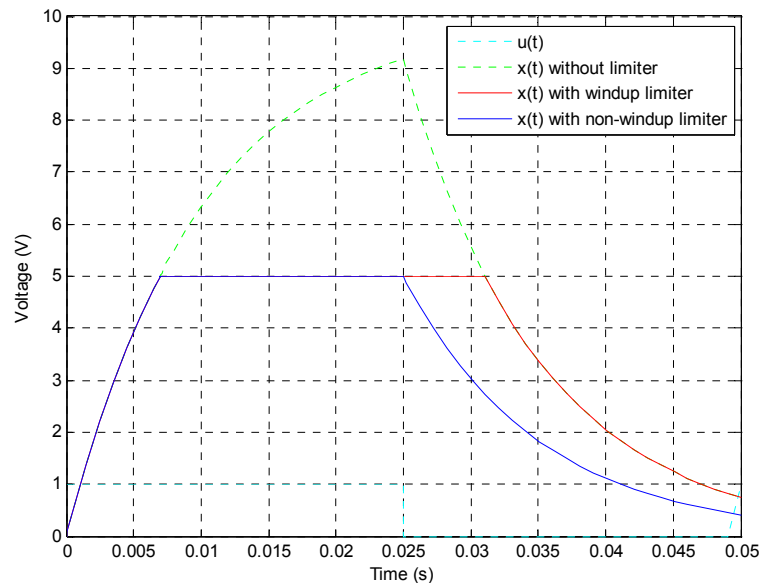


FIGURE 17: Transient response for a first-order transfer functions with windup and non-windup limiter

5.3.2 Single time constant block with non-windup limiter.

Single time constant block with non-windup limiter representation, its implementation and the equations that define its behaviour are shown in Figure 18. The main issue is to control the switch f , to let it open or closed according to the behaviour represented by the characteristic equations of the block.

The modelling of the single time constant block with non-windup limit in Simulink is shown in Figure 19. The control of the switch is made with a multiplication block that multiplies the outputs of the first gain block $1/T$ by the results of the groups of comparison and logical blocks that check the conditions of the equations of the limiter. So, in this case, the output of the multiplier block will be different to zero just when the output of the integrator block was between both limits and there was no change of sign for the function f . The constant T_A hasn't been included in the function f because it would modify only the magnitude of the function, not sign.

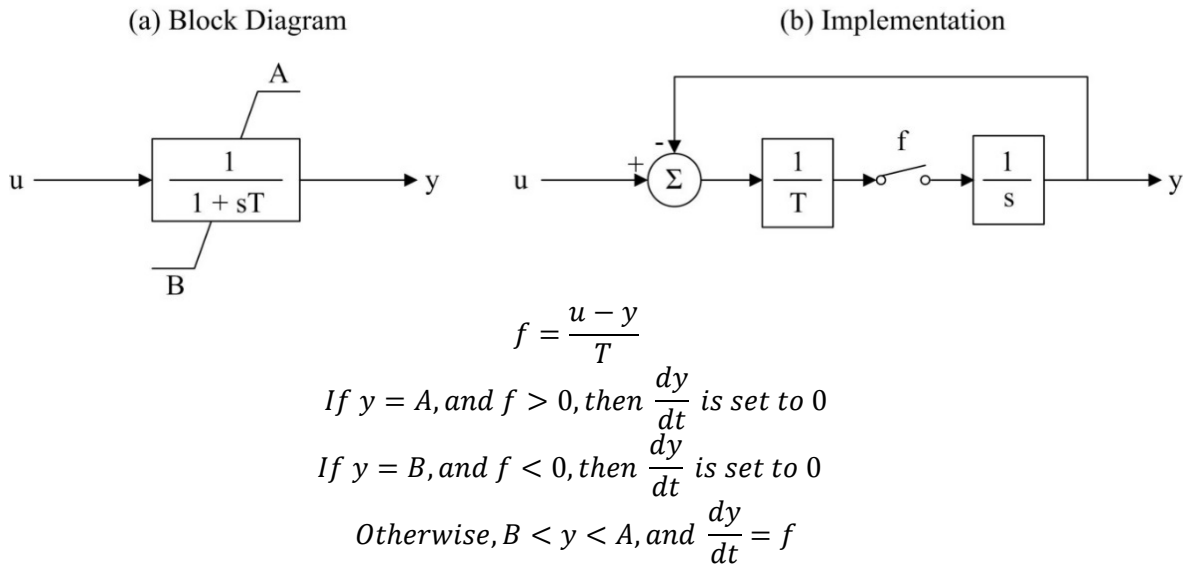


FIGURE 18: Single time constant block with non-windup limiter (IEEE, 1992)

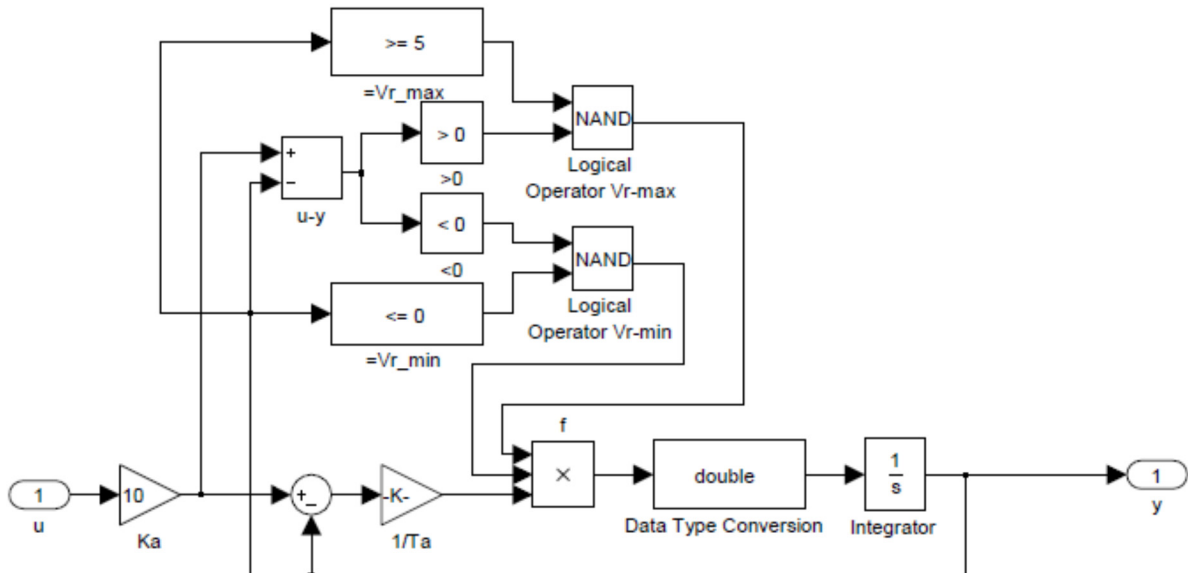
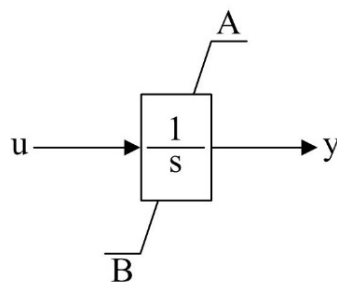


FIGURE 19: Single time constant block with non-windup limiter modelling in Simulink

5.3.3 Integrator block with non-windup limiter

The Integrator block with non-windup limiter representation, and the equations that define the behaviour of the limiter are shown in Figure 20. Basically, if the output is within the limits the integral action works normally, but when the output reaches the upper or lower limits the integral action is turned off and the output is held to the reached limit.



If $A \geq y \geq B$, then $\frac{dy}{dt} = u$

If $y > A$, then $\frac{dy}{dt}$ is set to 0

If $y < B$, then $\frac{dy}{dt}$ is set to 0

FIGURE 20: Integrator block with non-windup limiter (IEEE, 1992)

There are two ways of modelling this block; the first one is by the integrator block of the Simulink library, which includes the option of limiting it in the dialog box of the block. This limiter works as a non-windup limiter. The other way is to model it in a similar way of the single time constant block, by multiplying the input by the results of the groups of comparison and logical blocks that checks the conditions of the equations of the limiter. The modelling of the integrator block with non-windup limit in Simulink is shown in Figure 21.

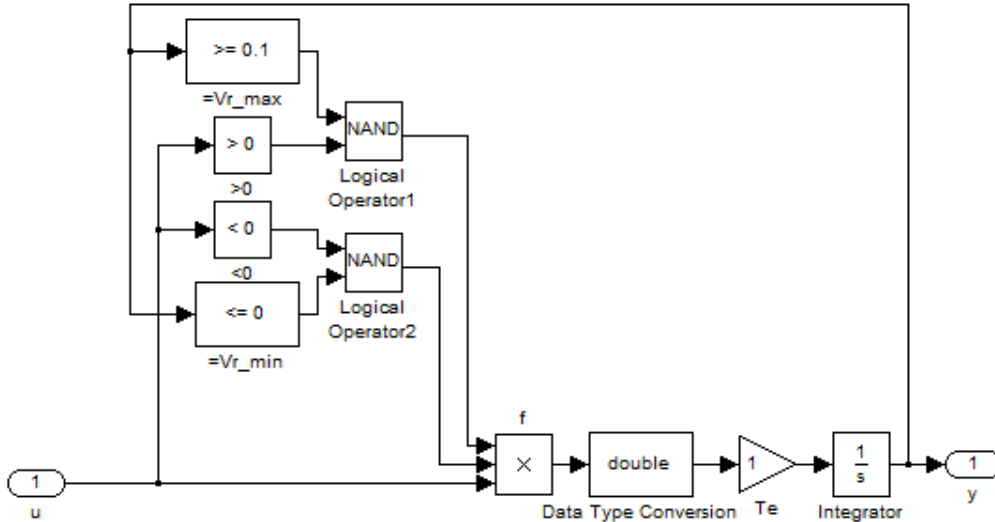


FIGURE 21: Integrator block with non-windup limiter modeled in Simulink

5.3.4 F_{EX} block

Figure 12 shows the equations that define the behaviour of the F_{EX} block in the AC1A excitation system. The output of the block F_{EX} depends on the value of the input I_N according to the characteristic equations. The modelling of the block was made basically with *Fcn block* of Simulink library, where basically the output is equal to a mathematic expression applied to the input. This expression is defined by the user. The mathematics equations that define the block are created. Then, a comparison and logical blocks define the range of values of the input; it will define the mathematic equation to be applied for the output. Finally, all options are added with a sum block. If the input is in a particular range of values, all other options will be zero. Figure 22 shows the modelling of F_{EX} block in Simulink.

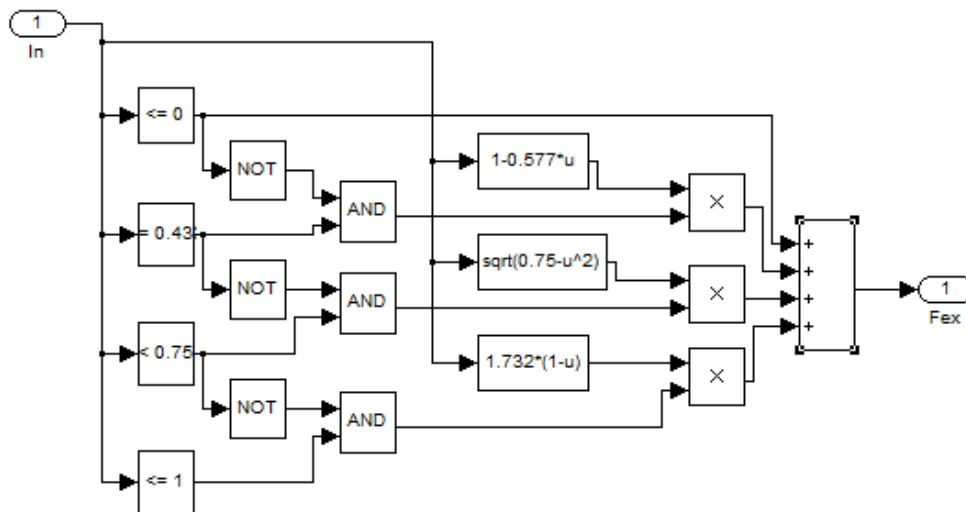


FIGURE 22: F_{EX} block modelling in Simulink

Finally, the complete AC1A and DECS-200 excitation systems modelling in Simulink are shown in Figures 23 and 24, respectively.

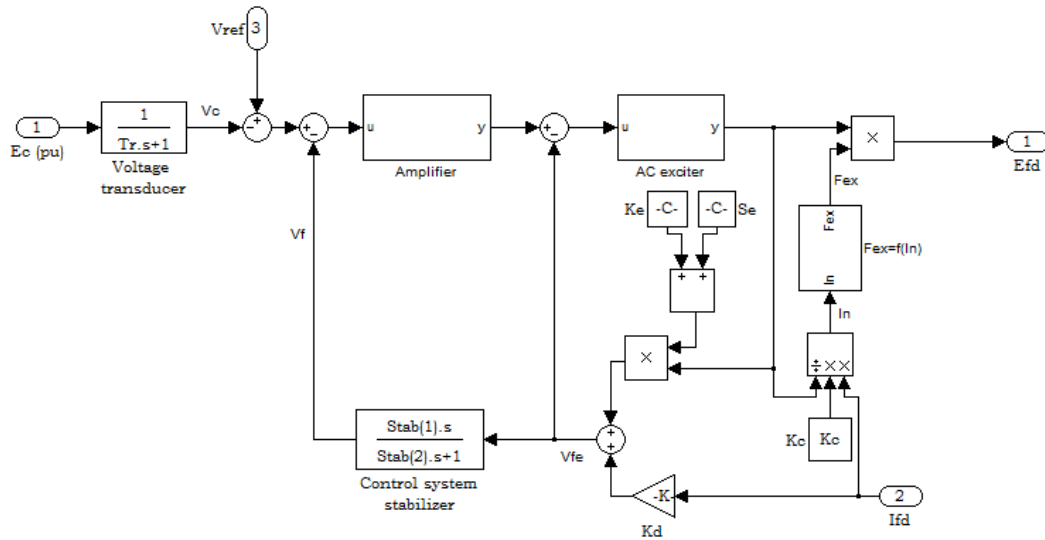


FIGURE 23: AC1A excitation system modelling in Simulink

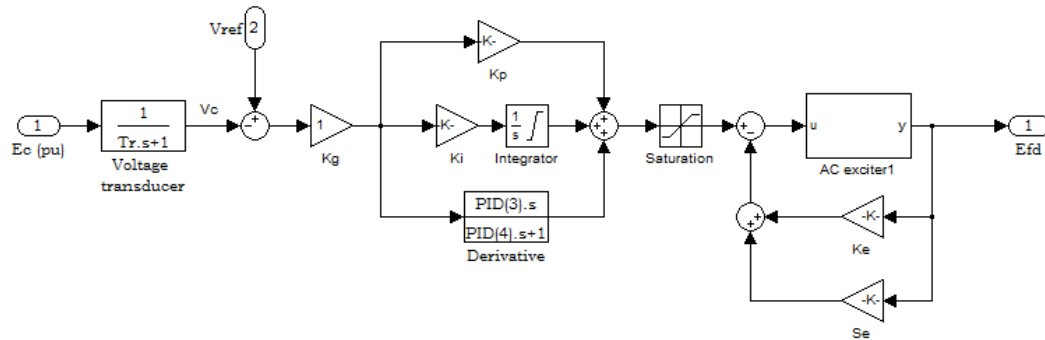


FIGURE 24: DESC-200 excitation system modelling in Simulink

5.4 Governor modelling

Governor has been modelling through the transfer functions in Simulink. Figure 10 shows turbine-governor transfer function modelled in this project. Excitation system basically has been modelled by simple transfer functions, integrators and math operation blocks. There is a single time constant block with non-windup limiter ($1/1+sT_1$) in the transfer function that represent the control valve for the steam input, but this block was modelled in the same way as described in 5.3.2. Figure 25 shows the turbine-governor modelling in Simulink.

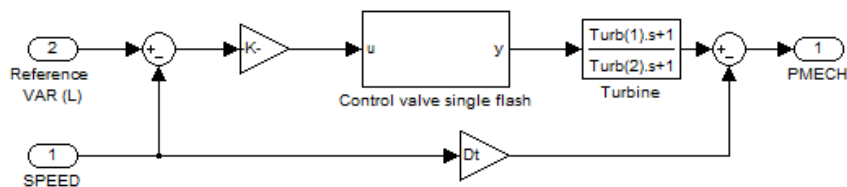


FIGURE 25: TGOV1 turbine-governor modelling in Simulink

Single time constant block and integrator block with non-windup limiter have been modelling inside a subsystem block, which is a block of Simulink library which represents a subsystem of the system that contains it. Because of that, in Figures 23, 24 and 25, they are simple blocks (AC exciter, Amplifier and Control valve single flash) that contain the complete models shown in Figures 21 and 22. The same have been done with the entire excitation system model and turbine governor model, which will be shown just as simple blocks in the model of each generator unit group later in this document.

6. SIMULATION RESULTS

Simulation and modelling for the stability analysis in CGB have been realized based on the cases detailed in Table 4. Different figures with plots of the most important variables of the system will be shown, as well as calculation of eigenvalues and other important properties. For base case, the plots of field voltage, stator voltage, Turbine-governor mechanical power, rotor speed, load angle, active power, and reactive power for each generator, will be shown.

For cases 1 to 6, the plots of rotor speed, load angle, stator voltage, and normalized eigenvectors for each unit, will be shown. To normalize eigenvectors, the one with highest magnitude is chosen as the reference and all of them, magnitude and angle, are divided by the reference eigenvector. Additionally, the eigenvalues, the damping ratio, and the frequency of oscillation, have been calculated. The eigenvalues and eigenvectors have been calculated by the Prony analysis described in 4.7.5, using the rotor speed signal for the analysis.

6.1 Base case simulation

Base case basically shows the behaviour of the system without any contingency. The simulation time is 75 seconds. During the first seconds of the simulation, the system is not in a stable state because of initial conditions. After approximately 40 seconds, the system becomes stable. Figure 27 shows the model in Simulink for base case.

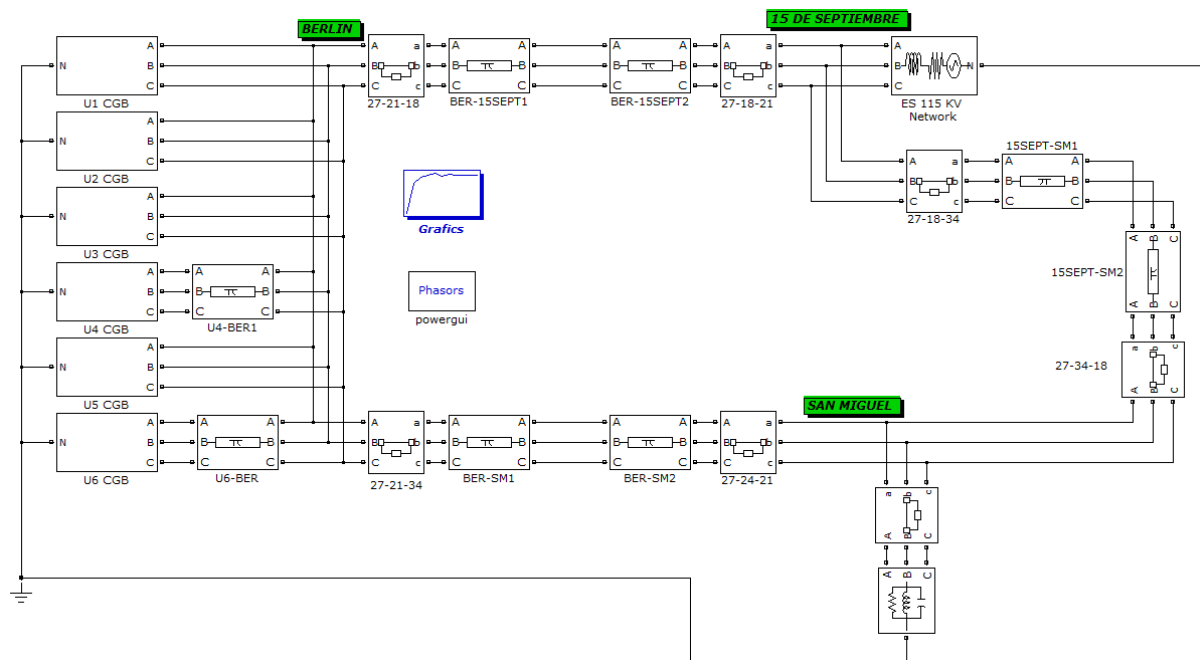


FIGURE 27: CGB base case modelling in Simulink

6.1.1 Field voltage and Stator voltage plots

Figures 28 and 29 show the field voltage and stator voltage for all generating units of CGB for base case. It can be seen an oscillating condition during the first 8 seconds because of the initial conditions of the system, but after that it stops to oscillate and tends to return to a stable state.

6.1.2 Turbine-governor Mechanical Power

Figure 30 shows the Turbine-governor mechanical power of CGB for base case. Like the same model of turbine-governor has been applied for all generators, the output characteristics are basically the same,

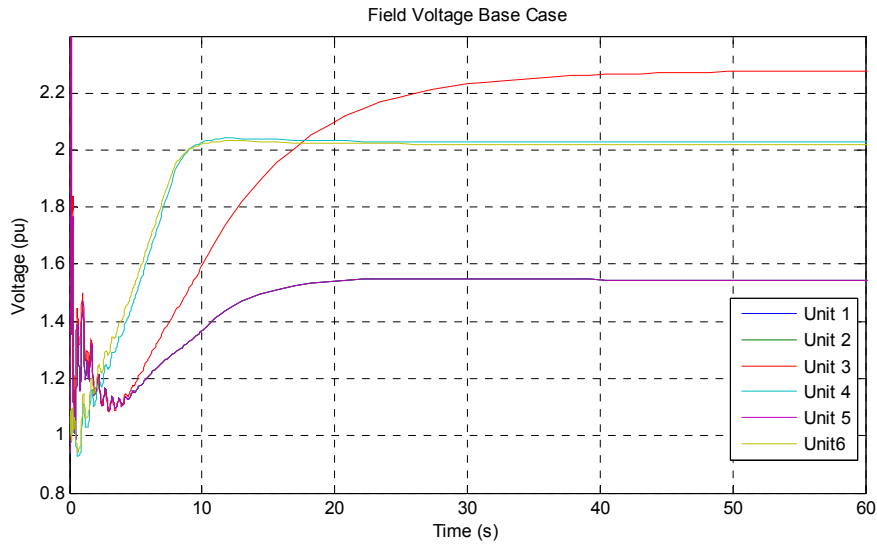


FIGURE 28: Field voltage CGB base case

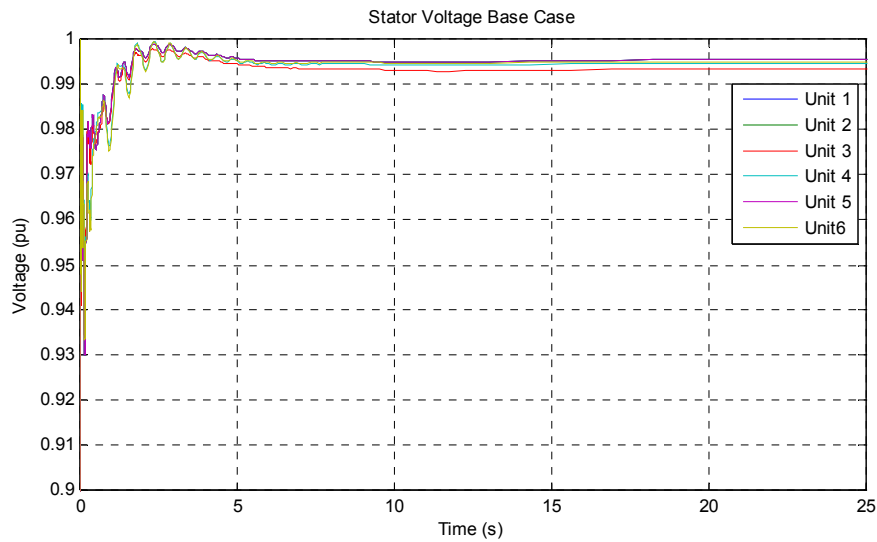


FIGURE 29: Stator voltage CGB base case

so in the figure all plots have basically the same behaviour. The stable state is reached at 40 seconds approximately.

6.1.3 Rotor Speed

Figure 31 shows the rotor speed of CGB for base case. Just the first 10 seconds are shown because after that time, the rotor speed becomes stable. The speed oscillations are just during the firsts 5 seconds because of the initial conditions.

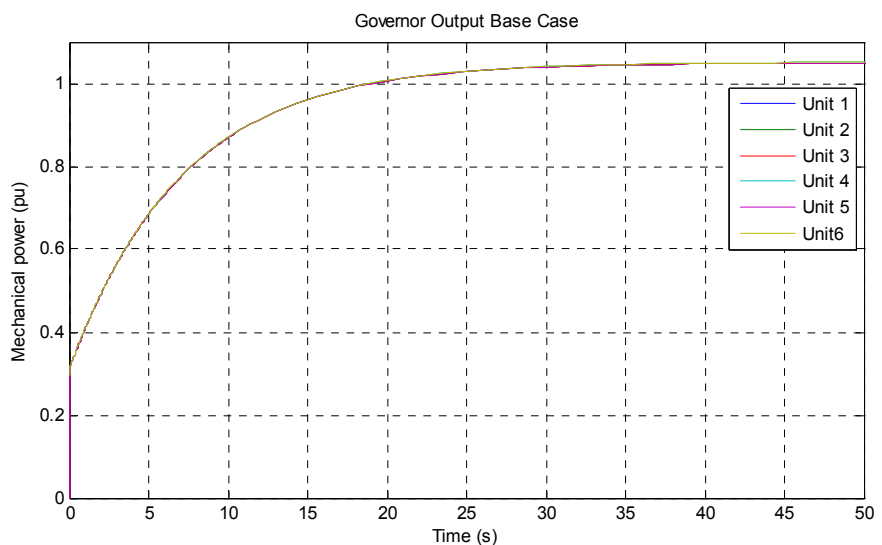


FIGURE 30: Turbine-governor mechanical power CGB base case

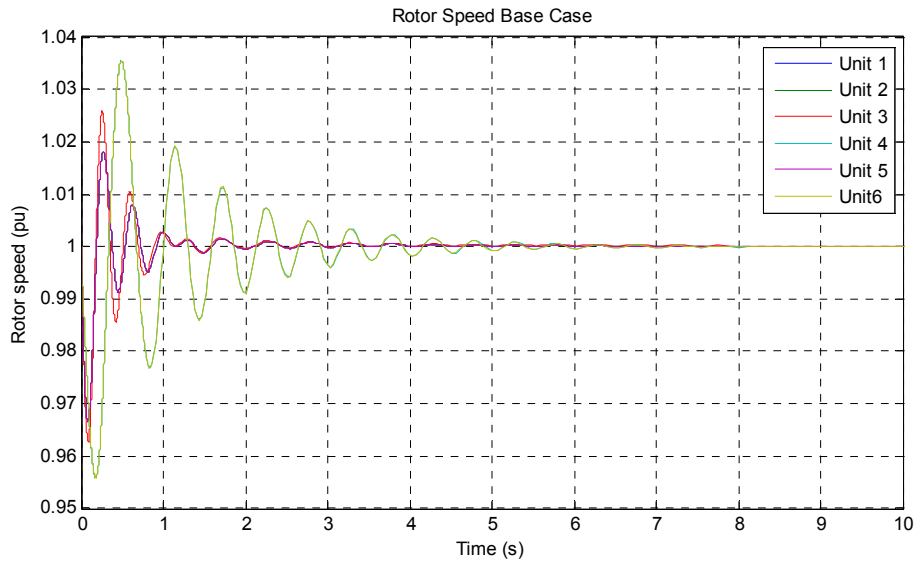


FIGURE 31: Rotor speed CGB base case

6.1.4 Load angle

Load angle shows the rotor angle of each machine respect to the load of the system. All load angles are lower than 90° , which indicates that power transfer has not reached the maximum value. Figure 32 shows the load angles for all generators.

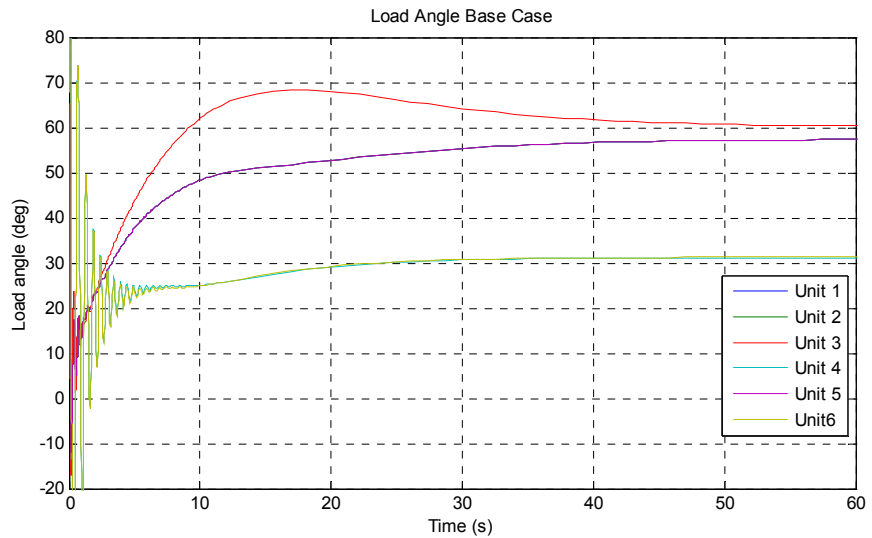


FIGURE 32: Load angle CGB base case

6.1.5 Active and reactive power

Figures 33 and 34 show the active and reactive power plots for each generator. The power output depends on the power demand on the network and the infinite bus characteristic.

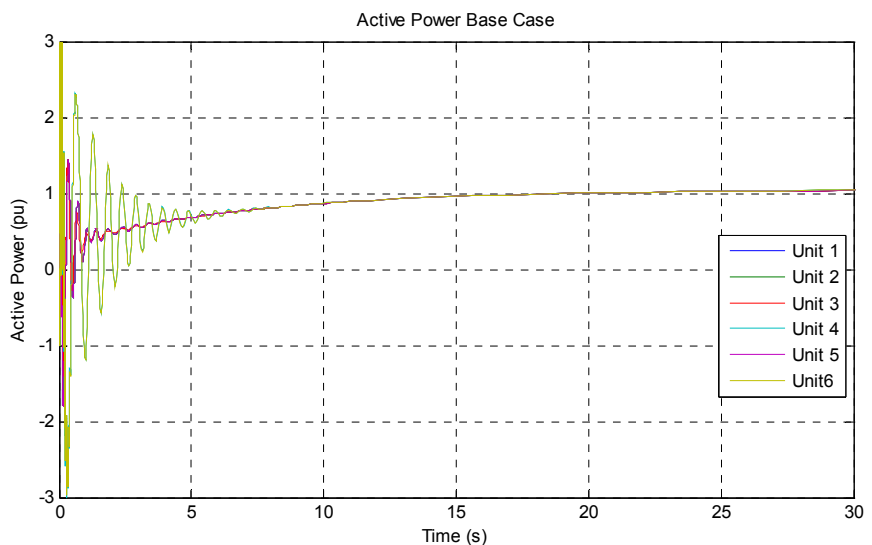


FIGURE 33: Active power CGB base case

6.2 Case 1 Modelling

Case 1 modelling includes the same model of base case but there has been added a 3-phase short circuit in the transmission line Berlin - 15 de Septie-mbre. Also included is the

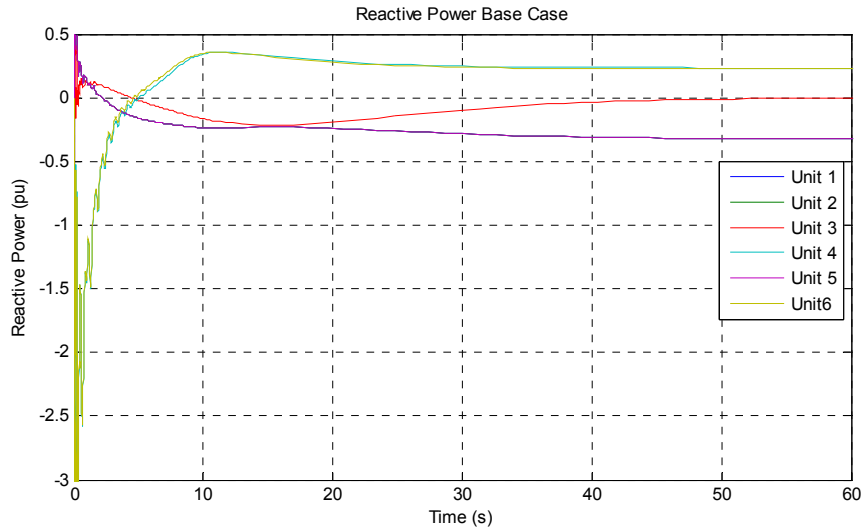


FIGURE 34: Reactive power CGB base case

operation of the circuit breakers in both ends of the line to clean the fault. The fault occurs at 75 seconds to let the systems be in steady state at the fault occurrence and the circuit breakers operate at 75.1 seconds. The total simulation time is 120 seconds, to let the system to reach steady state again after the fault. Figure 36 shows the complete system modelling in Simulink for case 1.

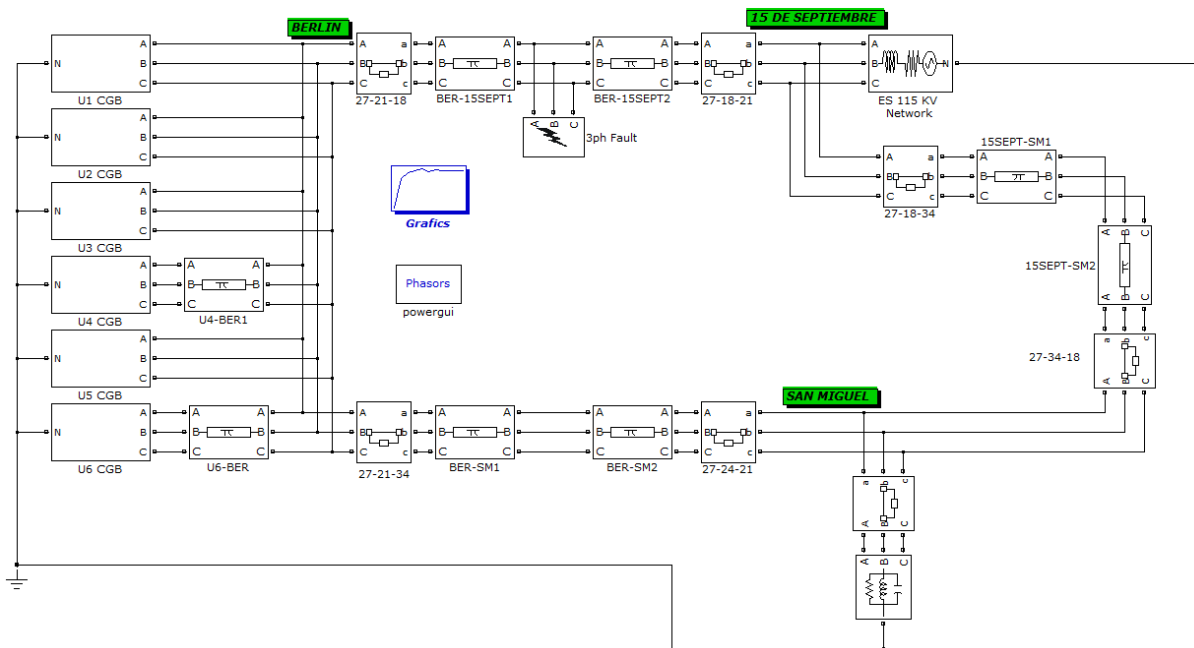


FIGURE 35: CGB Case 1 modelling in Simulink

6.2.1 Rotor speed

Figure 36 shows the rotor speed during the fault for case 1. It can be seen in the plots that the highest oscillation are for unit 4 and unit 6, with a deviation of 0.034 pu respect to nominal speed. It takes approximately 10 seconds after the fault occurrence to return to steady state.

6.2.2 Load angle

Figure 37 shows the load angle plots before, during and after the fault. Load angle change because of network configuration change. Basically the loss of transmission line causes changes in the impedances

of the system, excitation system and governor of each generator try to re-accommodate the abnormal condition for each generator and this causes the load angle change.

For unit 1, unit 2 and unit 5 the load angle before the fault is 57.39° and after the fault, for steady state, it change to 48.21° . For unit 3 the load angle change is for 60.22° to 52.82° and for units 4 and unit 6 there are practically no change, for 31.17° to 31.03° .

6.2.3 Stator voltage

Figure 38 shows the behaviour of stator voltage during the fault for case 1. Practically, the voltage collapse close to 0.1 pu during the fault and it starts to recover after the operation of the circuit breakers to clean the fault. Figure 39 makes a closer view of the stator voltage during the fault occurrence time, to show two different phenomena causing instability, first one is the 3-phase SC and, after 75.1 seconds, the effect of the operation of circuit breakers.

6.2.4 Eigenvalues and eigenvectors.

Table 5 shows the eigenvalues and normalized eigenvectors calculated by Prony Toolbox in Simulink for case 1. The table shows damping ratio and frequency of oscillation. Additionally, Figure 40 shows the eigenvectors plot. The magnitude of an

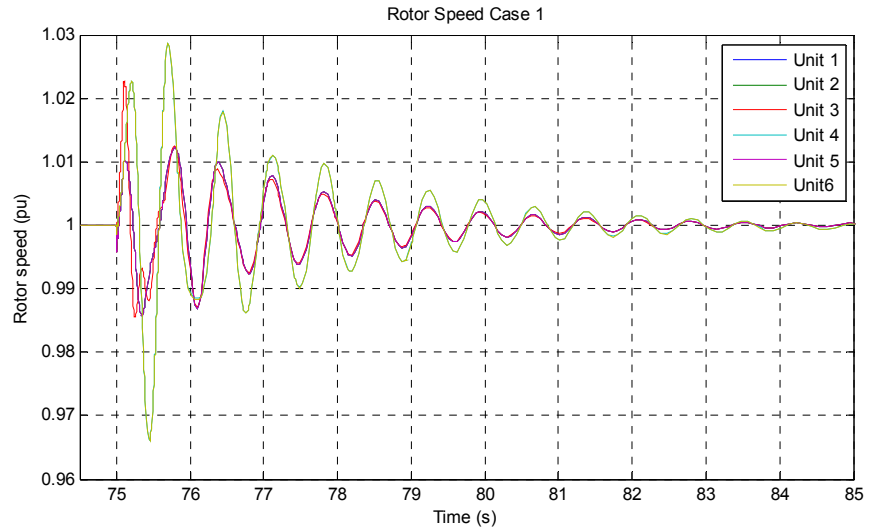


FIGURE 36: Rotor speed CGB case

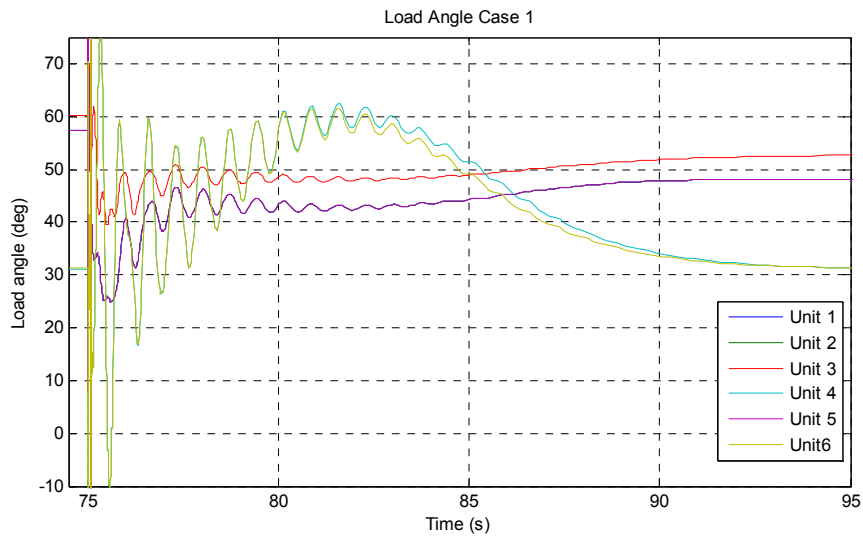


FIGURE 37: Load angle CGB case 1

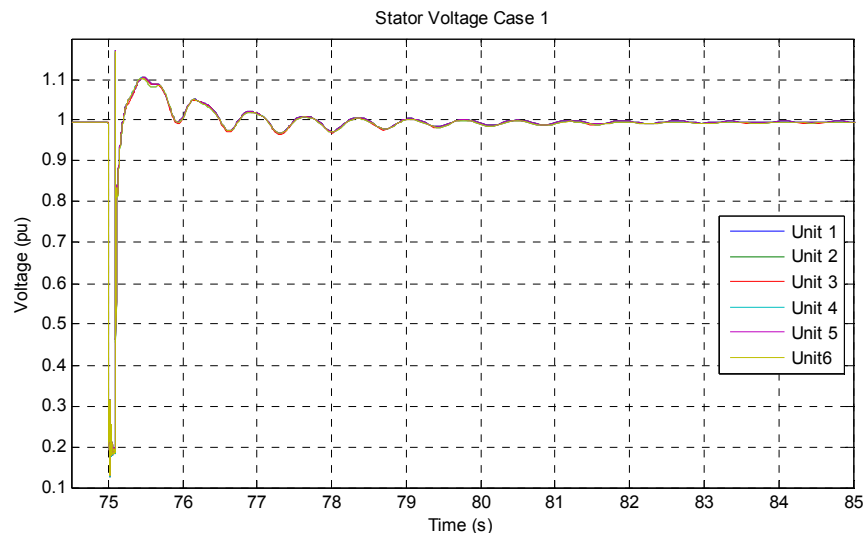


FIGURE 38: Stator voltage CGB case 1

eigenvector corresponds to the degree of influence for the specific vector to the oscillation, higher magnitude leads to higher oscillation contribution.

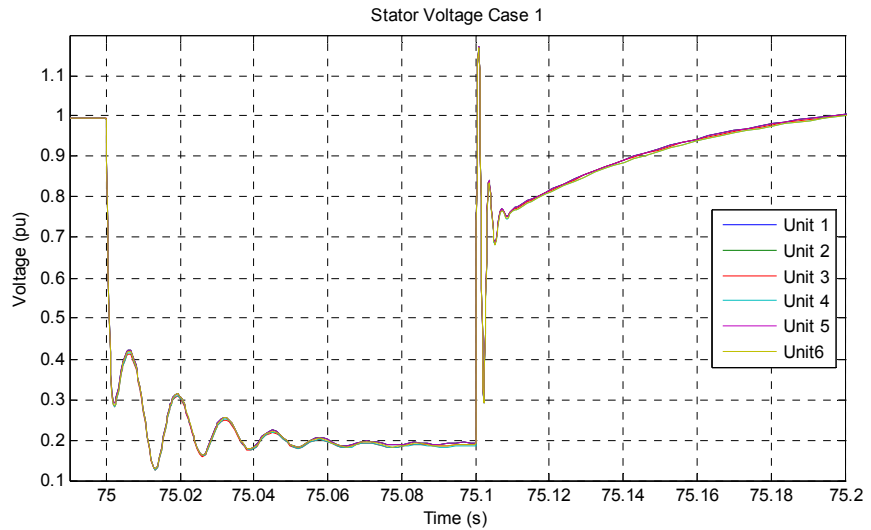


FIGURE 39: Stator voltage during fault occurrence for case 1

TABLE 5: Eigenvalues, eigenvectors, frequency and damping ratio for case 1

Generator	Eigenvalues		Eigenvector		Frequency (Hz)	Damping ratio	Decay time (s)
	σ	ω	Magnitude	Angle ($^{\circ}$)			
Unit 1	-0.73	9.42	1	0	1.5	0.077	1.37
Unit 2	-0.73	9.42	1	0	1.5	0.077	1.37
Unit 3	-1.8	8.17	0.875	-5	1.3	0.215	0.56
Unit 4	-0.26	9.42	0.875	-1.27	1.5	0.028	3.85
Unit 5	-0.73	9.42	1	0	1.5	0.077	1.37
Unit 6	-0.26	9.42	0.875	-1.27	1.5	0.028	3.85

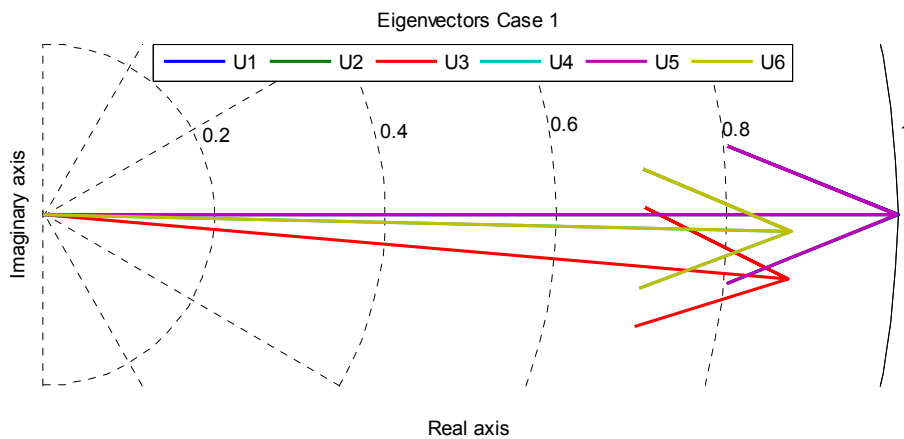


FIGURE 40: Eigenvectors case 1

6.2.5 Inherent stability

Inherent stability refers to the stability of each unit with respect of one chosen unit. Unit 3 has been chosen as the reference, because it has the highest load angle values. Then, we have plot the load angle difference for the other units. If these angle differences are below 90° then the units are inherently stable. Figure 41 shows inherent stability plot.

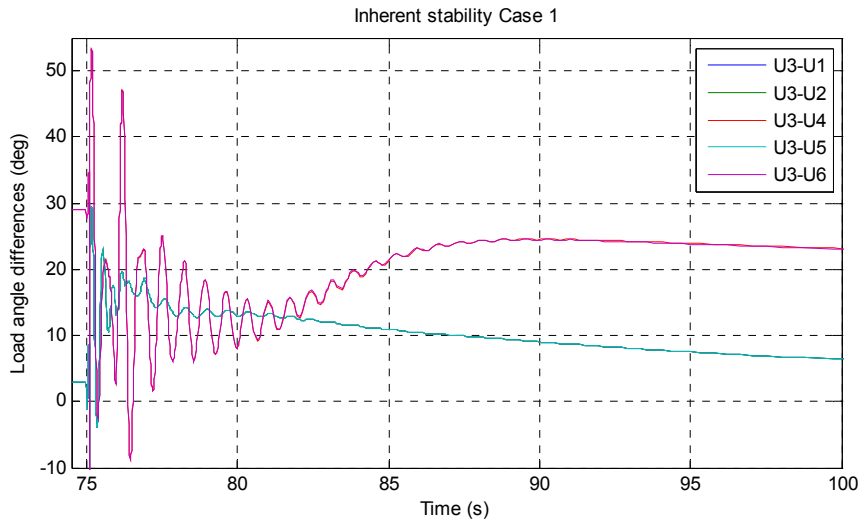


FIGURE 41: Load angle differences case 1

6.3 Case 2 modelling

For case 2 modelling have been added a 3-phase short circuit in the transmission line Berlin-San Miguel. Operation of the circuit breakers have been included in both ends of the line to clean the fault. The fault occurs at 75 seconds and the circuit breakers operate at 75.1 seconds. The total simulation time is 120 seconds. Figure 42 shows the complete system modelling in Simulink for case 2.

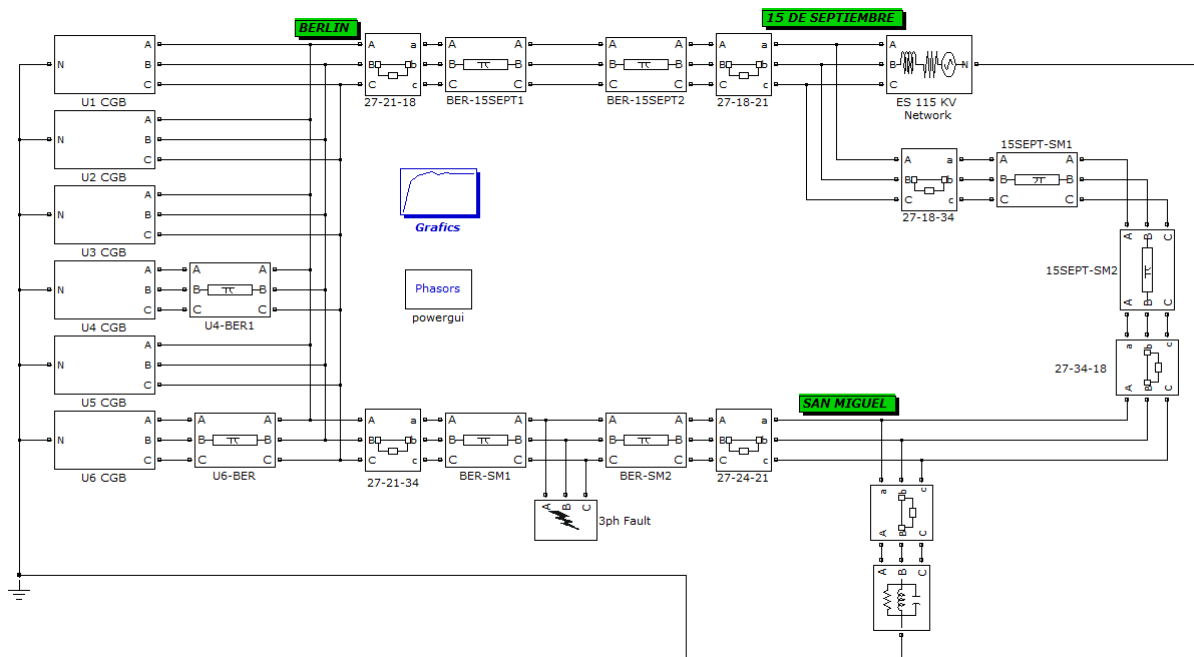


FIGURE 42: CGB case 2 modelling in Simulink

6.3.1 Rotor speed

Figure 43 shows the rotor speed during the fault for case 2. It can be seen in the plots that the highest oscillations are for unit 4 and unit 6 again, with a peak value of approximately 1.01 pu. However, the maximum deviation is 0.0123 pu, corresponding to unit 3, but the oscillations are lower for this unit. It takes approximately 5 seconds after the fault occurrence to return to a steady state.

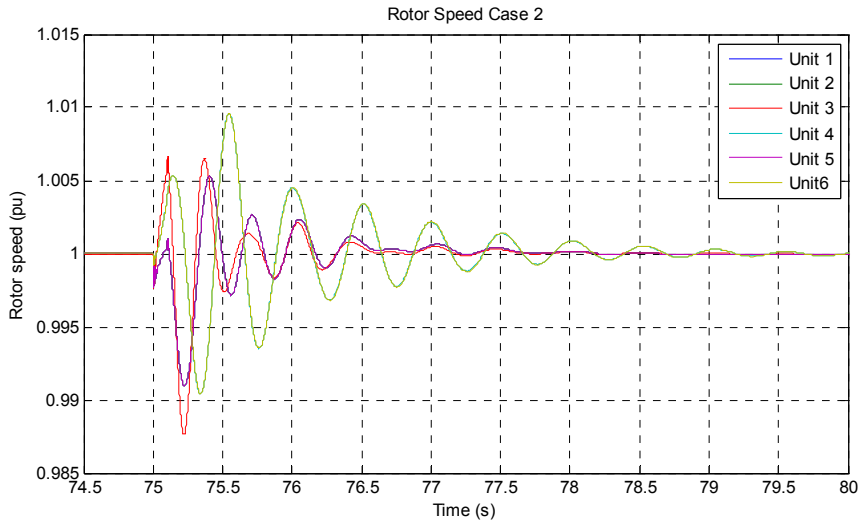


FIGURE 43: Rotor Speed CGB Case 2

6.3.2 Load angle

Figure 44 shows the load angle plot before, during and after the fault. Load angle changes for case 2 are much smaller than for case 1, because the load in the faulted line for this case is lower than faulted line for case 1. For unit 1, unit 2 and unit 5 the load angle before the fault is 57.39° and after the fault, for a steady state, it changes to 58.22° . For unit 3 the load angle change is for 60.22° to 60.69° and for units 4 and unit 6 the load angle change is 31.26° to 31.32° .

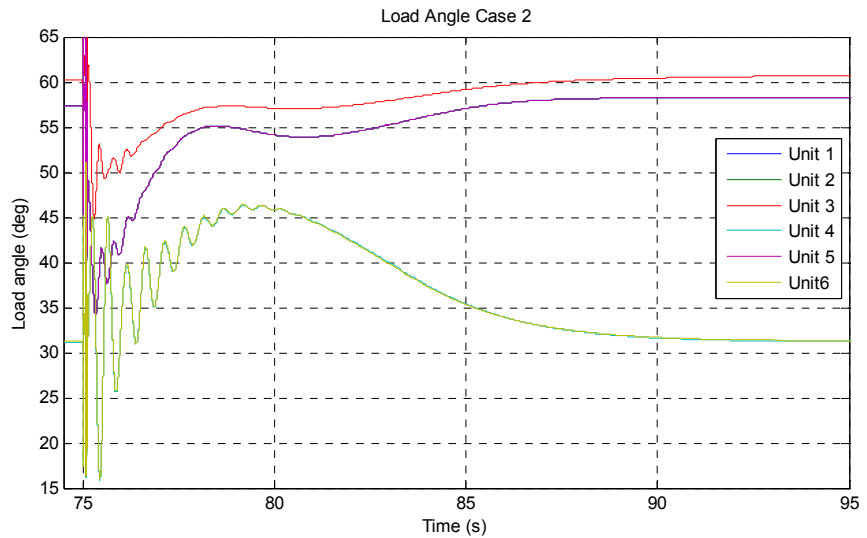


FIGURE 44: Load angle CGB case 2

6.3.3 Stator voltage

Figure 45 shows the behaviour of stator voltage during the fault. The voltage collapse is lower than case 1, close to 0.5 pu during the fault, and it starts to recover after the operation of the circuit breakers to clean the fault. Figure 46 shows a closer view of the stator voltage during the fault occurrence time; we can see the effect of the 3-phase SC first, and after 75.1 seconds, the effect of the operation of circuit breakers.

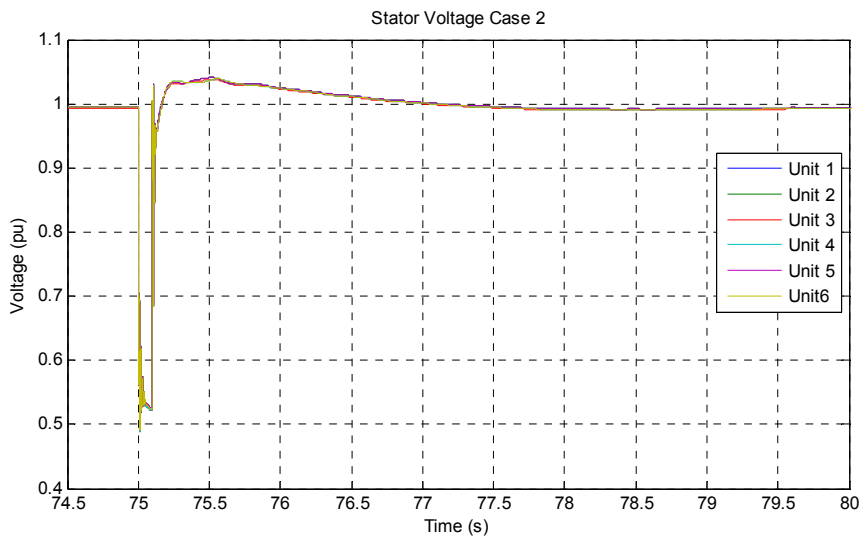


FIGURE 45: Stator voltage CGB case 2

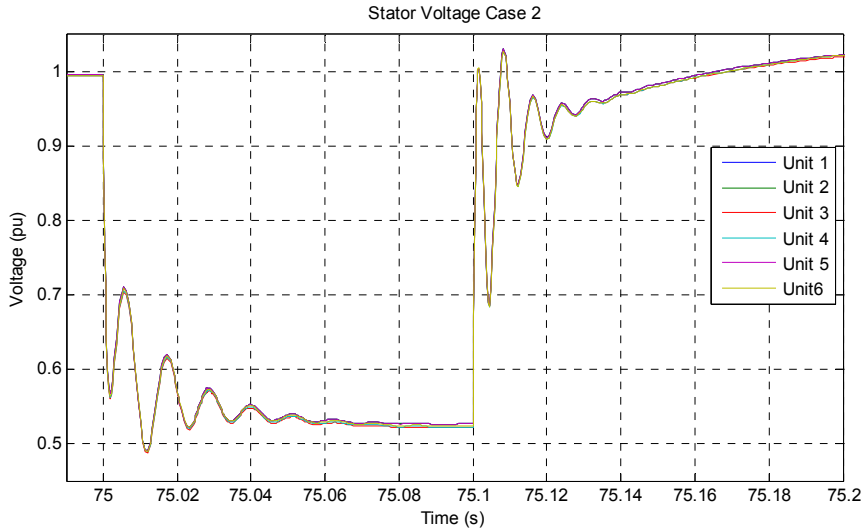


FIGURE 46: Stator voltage during fault occurrence for case 2

6.3.4 Eigenvalues and eigenvectors

Table 6 shows the eigenvalues and normalized eigenvectors for case 2 and Figure 47 shows the eigenvectors plot. In general, compared with case 1, damping values are bigger, that means that decay time will be smaller. Frequency is very similar for case 2, eigenvectors magnitudes are bigger, eigenvectors angles are very similar and damping ratio are bigger for all units.

TABLE 6: Eigenvalues, eigenvectors, frequency and damping ratio for case 2

Generator	Eigenvalues		Eigenvector		Frequency (Hz)	Damping ratio	Decay time (s)
	σ	ω	Magnitude	Angle (°)			
Unit 1	-8.3	10.05	0.821	-0.448	1.6	0.637	0.12
Unit 2	-8.3	10.05	0.821	-0.448	1.6	0.637	0.12
Unit 3	-5.8	13.82	0.615	0.222	2.2	0.387	0.17
Unit 4	-1.6	12.57	1	0	2	0.126	0.63
Unit 5	-8.3	10.05	0.821	-0.448	1.6	0.637	0.12
Unit 6	-1.5	12.57	0.949	0.037	2	0.118	0.67

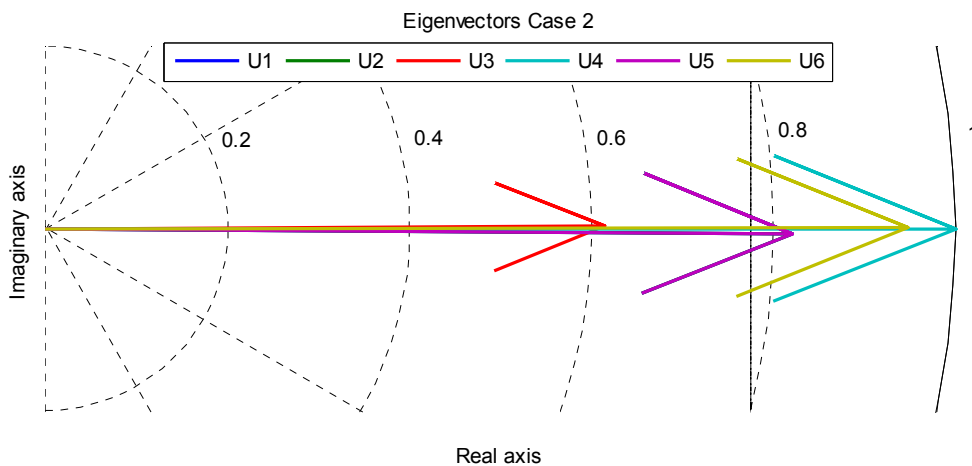


FIGURE 47: Eigenvectors case 2

6.4 Case 3 modelling

For case 3 modelling the 3-phase short circuit is located in the transmission line 15 de Septiembre - San Miguel. Operation of the circuit breakers have been included in both ends of the line to clean the fault. The fault occurs at 75 seconds and the circuit breakers operate at 75.1 seconds. Total simulation time is 120 seconds. Figure 48 shows the complete system modelling in Simulink for case 3.

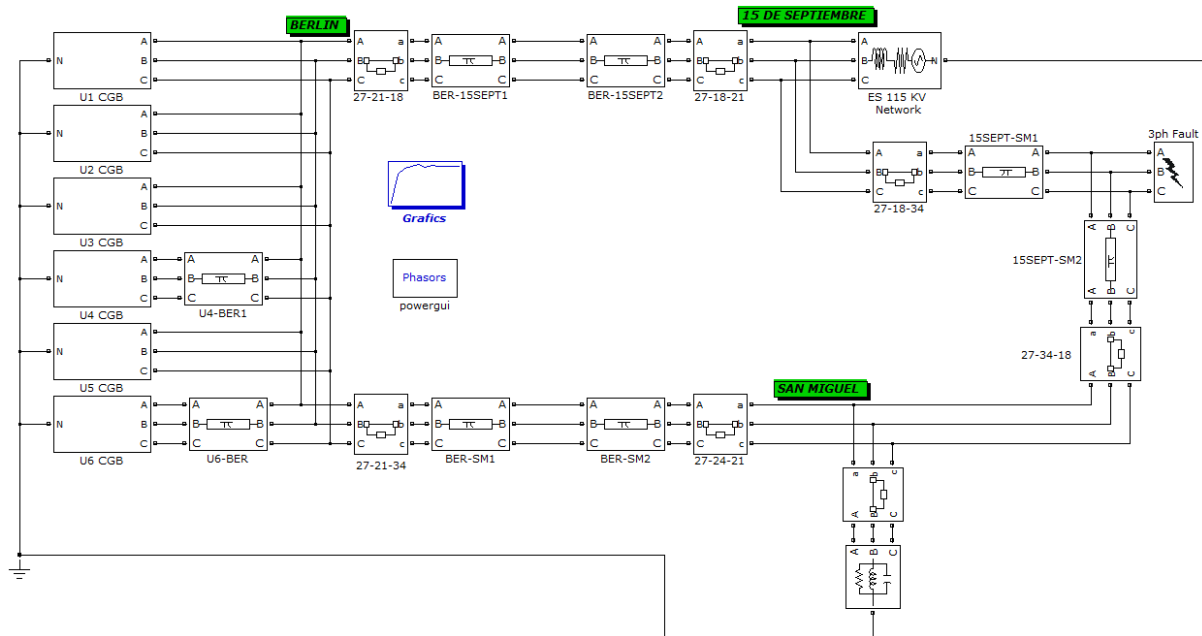


FIGURE 48: CGB Case 3 modelling in Simulink

6.4.1 Rotor speed

Figure 49 shows the rotor speed during the fault for case 2. It can be seen in the plots that the highest oscillations are for unit 4 and unit 6 again, with a peak value of approximately 1.008 pu. However, the maximum deviation is 0.0098 pu, corresponding to unit 3, but the oscillations are lower for this unit. It takes approximately 6 seconds after the fault occurrence to return to a steady state.

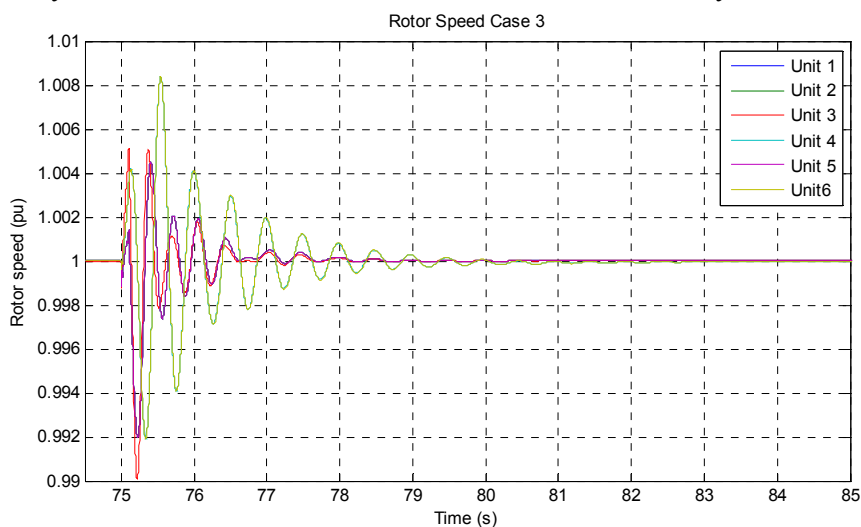


FIGURE 49: Rotor speed CGB case 3

6.4.2 Load angle

Figure 50 shows the load angle plot before, during and after the fault. Load angle changes for case 3 are a little higher than case 2, because the load in the line 15 de Septiembre-San Miguel is higher than load

at line Berlin-San Miguel. For unit 1, unit 2 and unit 5 the load angle before the fault is 57.39° and after the fault, for a steady state, it changes to 55.4° . For unit 3 the load angle change is for 60.22° to 58.52° and for units 4 and unit 6 the load angle change is 31.26° to 31.33° .

6.4.3 Stator voltage

Figure 51 shows the behaviour of stator voltage during the fault. The voltage collapse is lower than case 2, close to 0.64 pu during the fault, and it starts to recover after the operation of the circuit breakers to clean the fault. Figure 52 shows a closer view of the stator voltage during the fault occurrence time; we can see the effect of the three-phase SC first, and after 75.1 seconds, the effect of the operation of circuit breakers.

6.4.4 Eigenvalues and eigenvectors

Table 7 shows the eigenvalues and normalized eigenvectors for case 3 and Figure 53 shows the eigenvectors plot. In general, compared with case 1, damping is smaller for all units except for unit 4 and unit 6. Frequency is bigger for case 3, eigenvectors magnitudes and angles are smaller, damping ratios are very similar for all units except for unit 3.

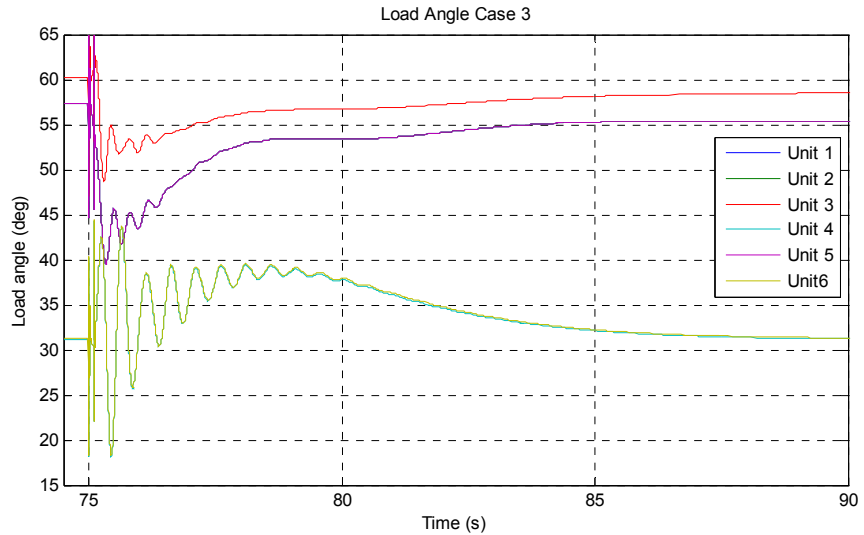


FIGURE 50: Load angle CGB case 3

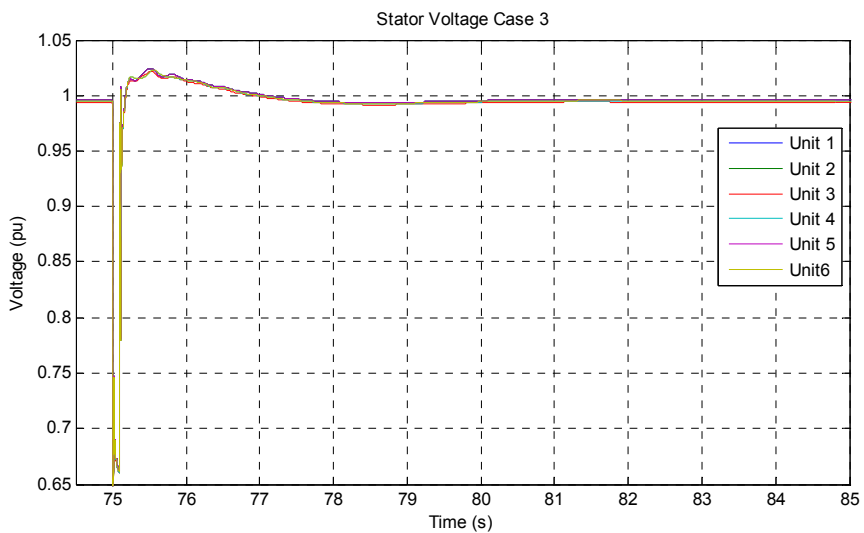


FIGURE 51: Stator voltage CGB case 3

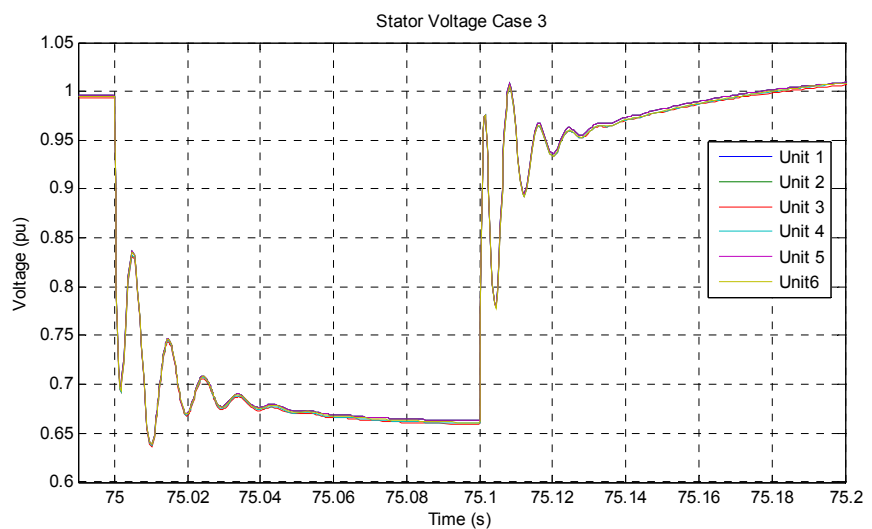


FIGURE 52: Stator voltage during fault occurrence for case 3

TABLE 7: Eigenvalues, eigenvectors, frequency and damping ratio for case 3

Generator	Eigenvalues		Eigenvector		Frequency (Hz)	Damping ratio	Decay time (s)
	σ	ω	Magnitude	Angle ($^\circ$)			
Unit 1	-0.37	19.48	0.173	0.038	3.1	0.019	2.7
Unit 2	-0.37	19.48	0.173	0.038	3.1	0.019	2.7
Unit 3	-1.2	18.85	0.182	0.023	3	0.064	0.83
Unit 4	-1.5	18.85	1	0	3	0.079	0.67
Unit 5	-0.37	19.48	0.173	0.038	3.1	0.019	2.7
Unit 6	-1.3	18.85	1	0	3	0.069	0.77

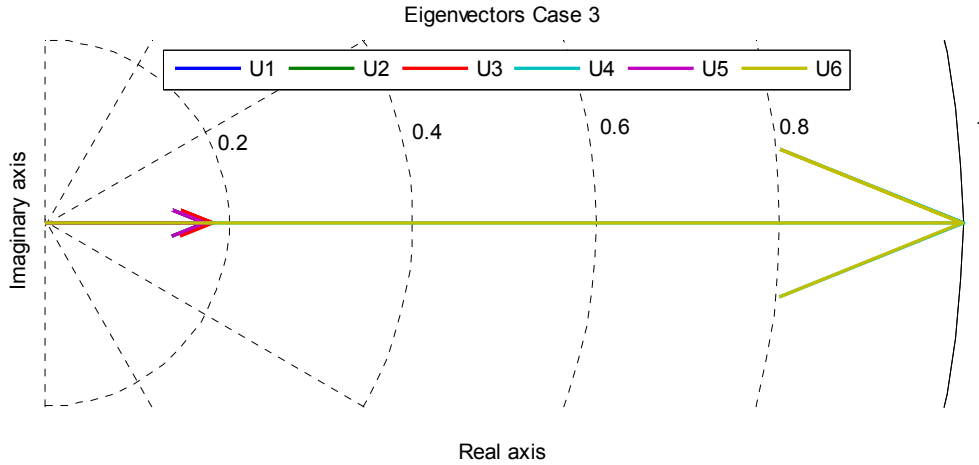


FIGURE 53: Eigenvectors case 3

6.5 Case 4 modelling

For case 4 modelling, there is a load increase of 55 MW at San Miguel bus. The load increase occurs at 75 seconds and this is the only small signal stability case, the other cases are transient stability. The total simulation time is 120 seconds. Figure 54 shows the complete system modelling in Simulink for case 4.

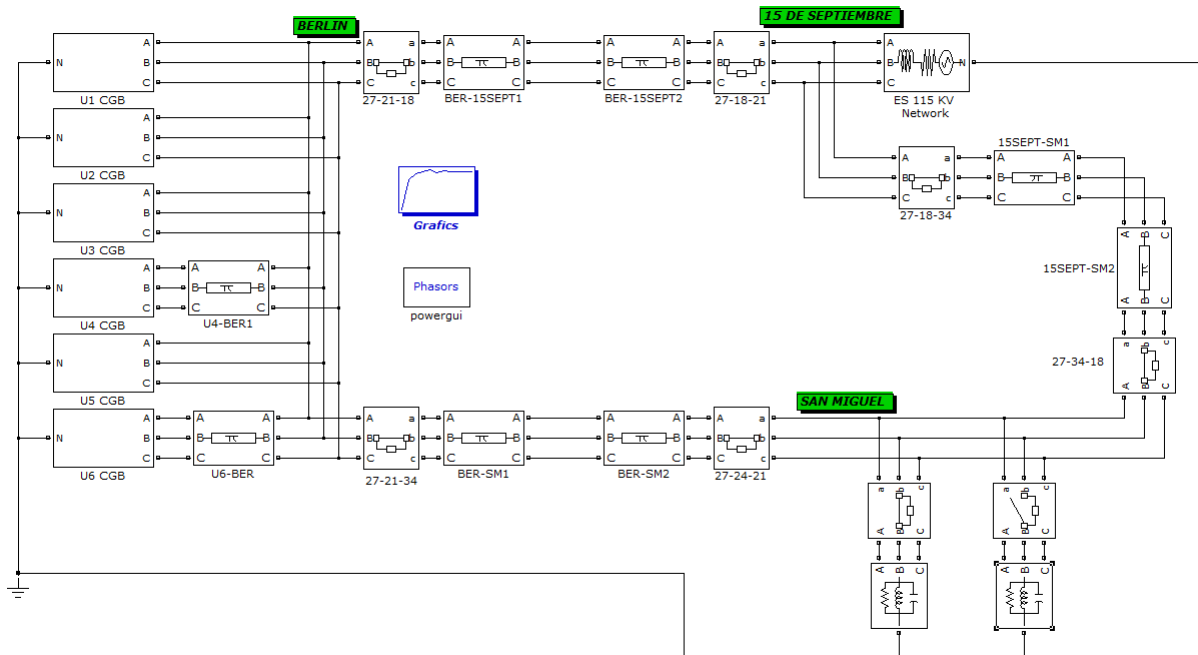


FIGURE 54: CGB case 4 modelling in Simulink

6.5.1 Rotor speed

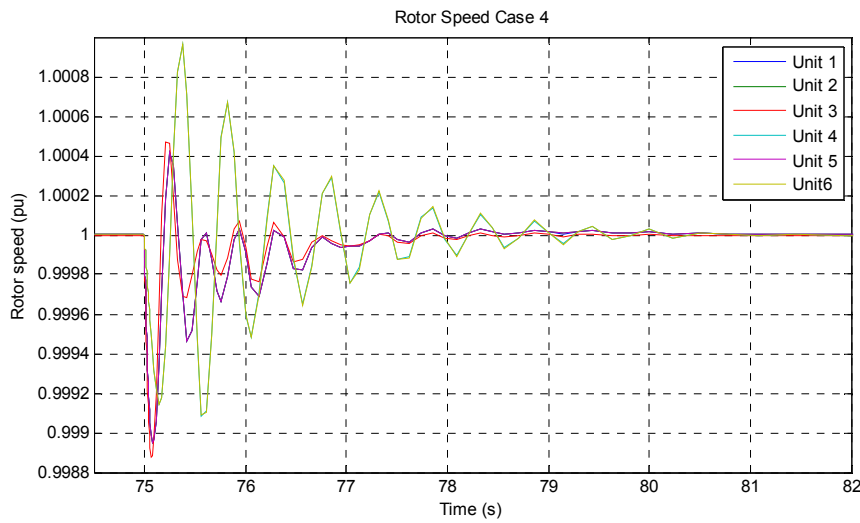


FIGURE 55: Rotor speed CGB case 4

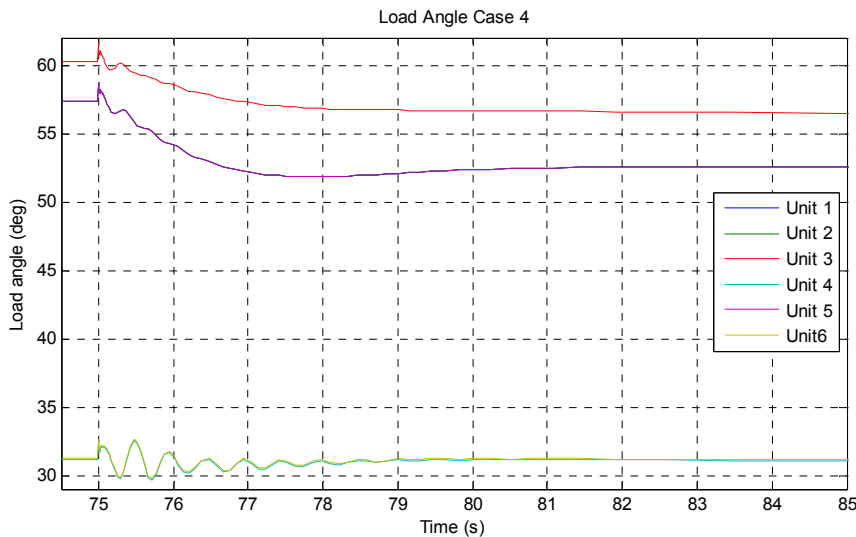


FIGURE 56: Load angle CGB case 4

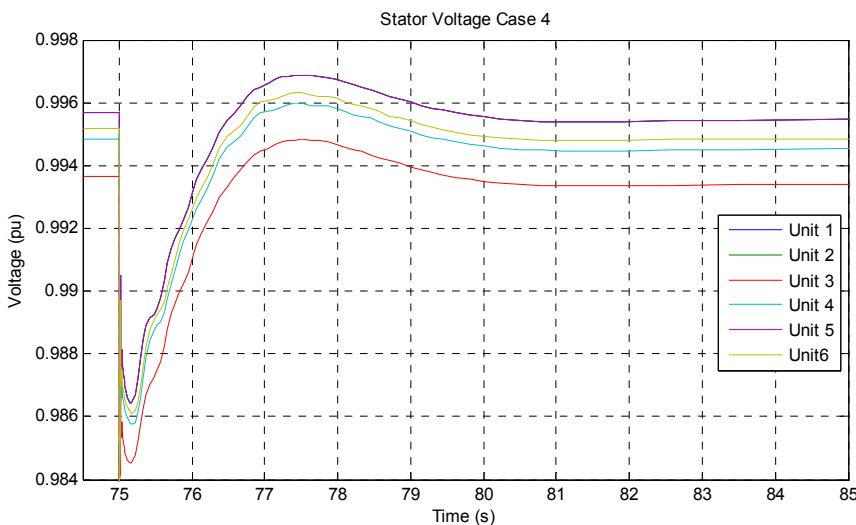


FIGURE 57: Stator Voltage CGB Case 4

Figure 55 shows the rotor speed during the load increase for case 4. It can be seen in the plots that the speed variation is much lower than for the previous cases. The highest oscillations are for unit 4 and unit 6 again, with a maximum deviation of -0.0008 pu. It takes approximately 3 seconds to return to a steady state.

6.5.2 Load angle

Figure 56 shows the load angle plot before, during and after the load increase. Load angle change behaviour for case 4 is different than previous cases, because oscillation are very small and takes just 5 seconds to go back to a steady state.

For unit 1, unit 2 and unit 5 the load angle before the load increase is 57.39° and after the load increase, for a steady state, it changes to 52.6° . For unit 3 the load angle change is 60.22° to 56.43° and for units 4 and unit 6 the load angle change is 31.26° to 31.15° .

6.5.3 Stator voltage

Figure 57 shows the behaviour of stator voltage during the fault. The voltage decrease is very low, around 0.98 pu and it goes back to a stable state in approximately 6 seconds. Figure 58 shows a closer view of the stator voltage during the load increase time and we only have the effect of the load increase for this case.

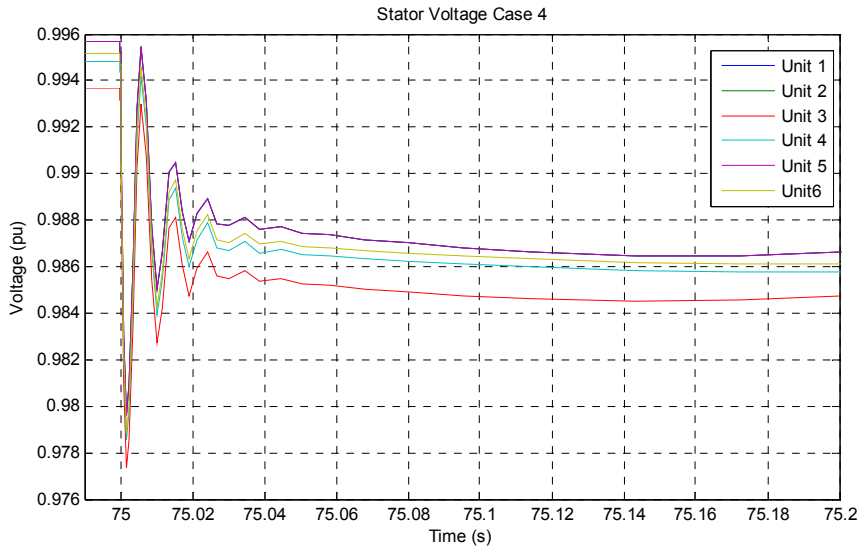


FIGURE 58: Stator voltage during load increase for case 4

6.5.4 Eigenvalues and eigenvectors.

Table 8 shows the eigenvalues and normalized eigenvectors for case 4 and Figure 59 shows the eigenvectors plot. In general, compared with case 1, damping and frequency are bigger for case 4. Eigenvectors magnitudes are very small, except for unit 4 and unit 6 and angles are positives. Damping ratios are smaller for all units except for unit 4 and unit 6, which are bigger.

TABLE 8: Eigenvalues, eigenvectors, frequency and damping ratio for case 4

Generator	Eigenvalues		Eigenvector		Frequency (Hz)	Damping ratio	Decay time (s)
	σ	ω	Magnitude	Angle ($^{\circ}$)			
Unit 1	-2.7	21.99	0.125	7.821	3.5	0.122	0.37
Unit 2	-2.7	21.99	0.125	7.821	3.5	0.122	0.37
Unit 3	-2.5	21.99	0.104	8.043	3.5	0.113	0.4
Unit 4	-8.5	19.48	1	0	3.1	0.4	0.12
Unit 5	-2.7	21.99	0.125	7.821	3.5	0.122	0.37
Unit 6	-8.6	19.48	1	0.029	3.1	0.404	0.12

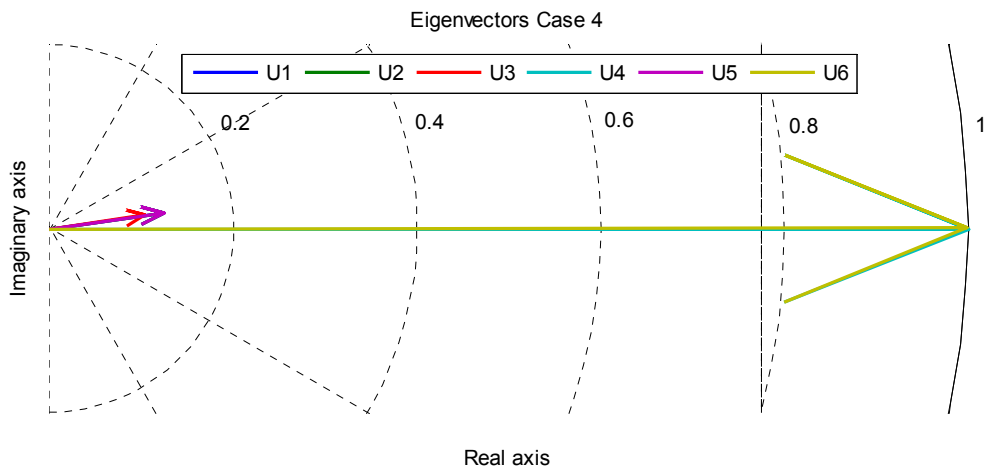


FIGURE 59: Eigenvectors case 4

6.6 Case 5 modelling

Case 5 modelling has a three-phase SC in line Berlin-15 de Septiembre, just like case 1, but the difference is that unit 3 is out of service. The 3-phase SC occurs at 75 seconds and circuit breakers operate at 75.1 seconds. The total simulation time is 120 seconds. Figure 60 shows the complete system modelling in Simulink for case 5.

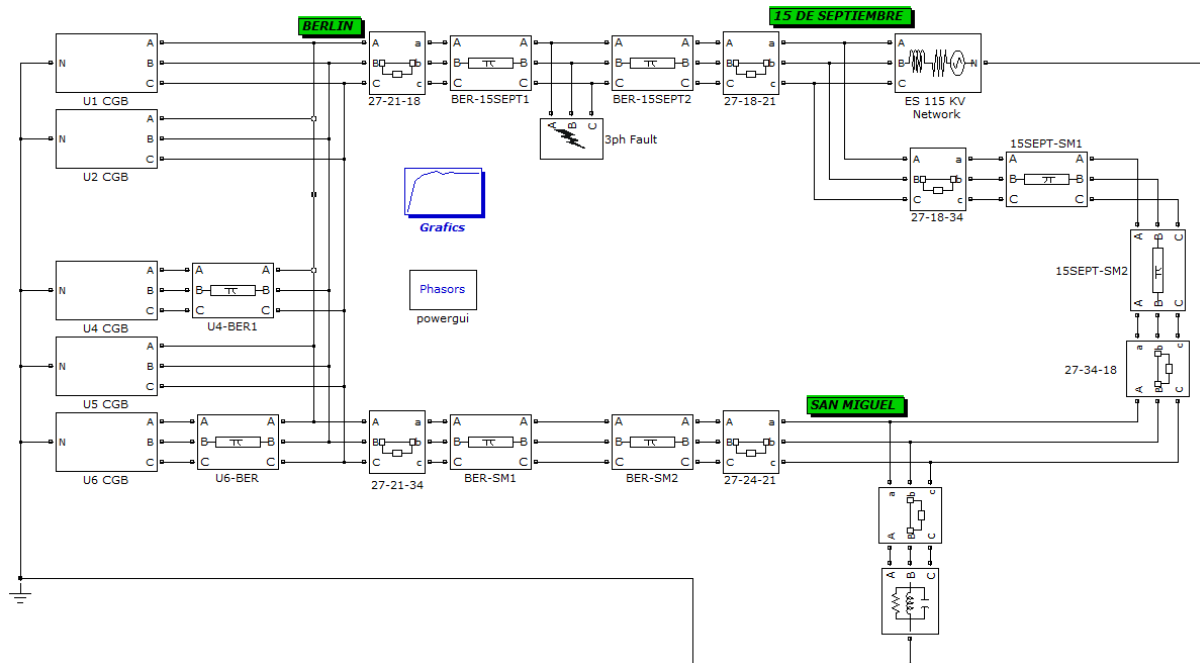


FIGURE 60: CGB case 5 modelling in Simulink

6.6.1 Rotor speed

Figure 61 shows the rotor speed during the load increase for case 5. It can be seen in the plots that the highest oscillation are for unit 4 and unit 6, with a maximum deviation of 0.0285 pu. The behaviour is very similar to case 1, with a slight reduction in oscillations amplitude. It takes approximately 7 seconds after the fault occurrence to return to steady state, 3 seconds less than case 1.

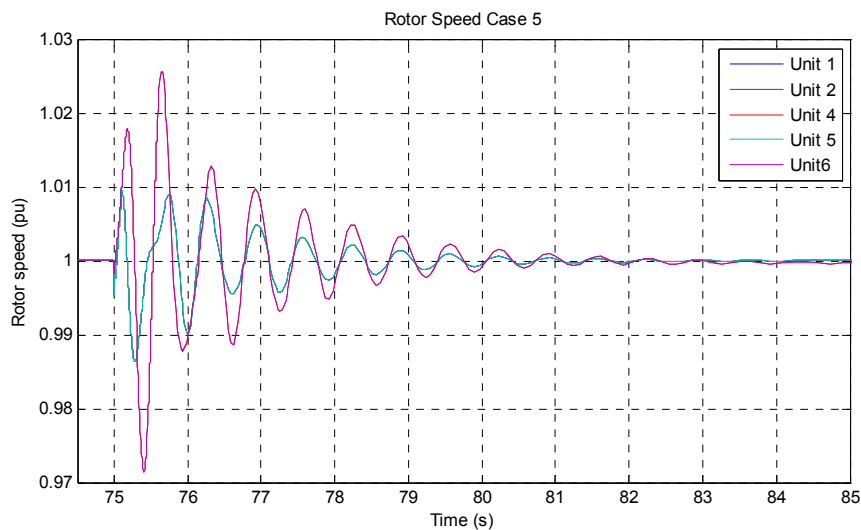


FIGURE 61: Rotor speed CGB case 5

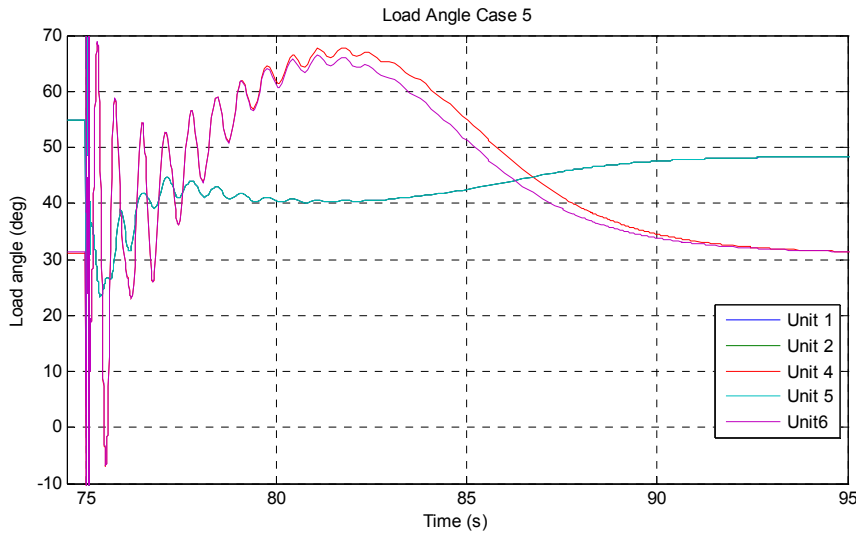


FIGURE 62: Load angle CGB case 5

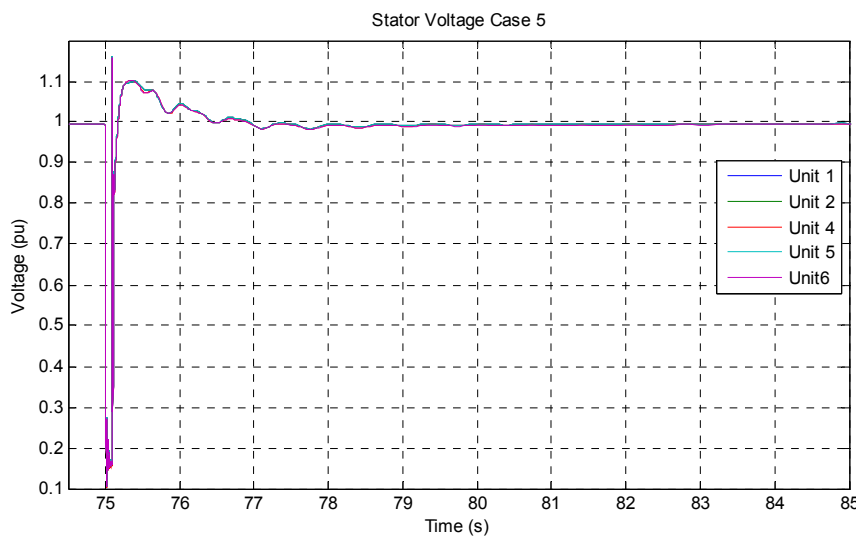


FIGURE 63: Stator voltage CGB case 5

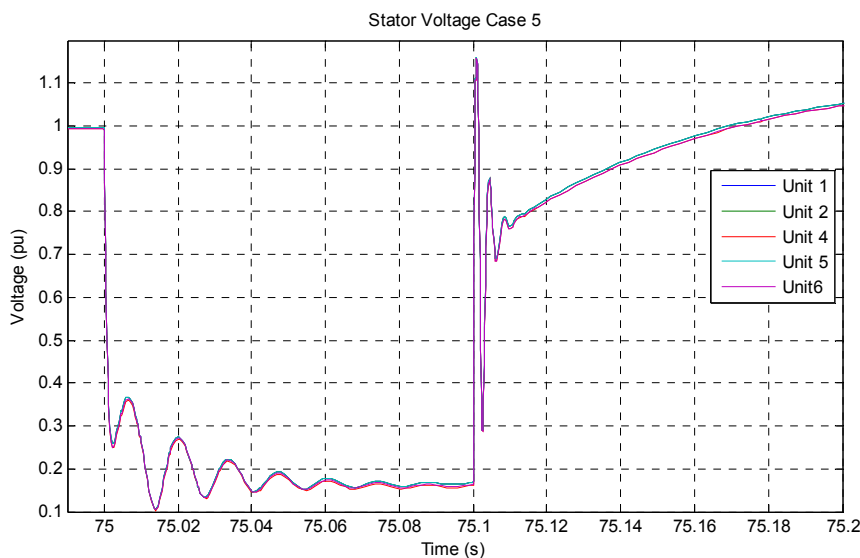


FIGURE 64: Stator voltage during fault occurrence for case 5

6.6.2 Load angle

Figure 62 shows the load angle plot before, during and after the fault. For unit 1, unit 2 and unit 5 the load angle before the fault is 54.87° and for unit 4 the load angle is 31.25° . There are small differences in load angle before the fault compared with case 1, because of different network configuration without unit 3. After the fault, for a steady state, the load angles are 48.34° for unit 1, unit 2 and unit 5, and 31.15° for unit 4 and unit 6.

6.6.3 Stator voltage

Figure 63 shows the behaviour of stator voltage during the fault. Practically, the voltage collapse close to 0.1 pu again, like in case 1, and it takes approximately 3 seconds to return to steady state, 2 seconds less than case 1. Figure 64 makes a closer view of the stator voltage during the fault occurrence time, to show the three-phase SC instability effect and, after 75.1 seconds, operation of circuit breakers effect.

6.6.4 Eigenvalues and eigenvectors

Table 9 shows the eigenvalues and normalized eigenvectors for case 4 and Figure 65 shows the eigenvectors plot. In general, compared with case 1, damping values are very similar but frequencies are bigger for case 5.

Eigenvectors magnitudes are bigger and all angles are very close to zero. Damping ratios are similar.

TABLE 9: Eigenvalues, eigenvectors, frequency and damping ratio for case 5

Generator	Eigenvalues		Eigenvector		Frequency (Hz)	Damping ratio	Decay time (s)
	σ	ω	Magnitude	Angle ($^\circ$)			
Unit 1	-0.53	6.91	0.486	0.25	1.1	0.076	1.89
Unit 2	-0.53	6.91	0.486	0.25	1.1	0.076	1.89
Unit 4	-0.6	6.28	1	0	1	0.095	1.67
Unit 5	-0.53	6.91	0.486	0.25	1.1	0.076	1.89
Unit 6	-0.59	6.28	1	-0.017	1	0.094	1.69

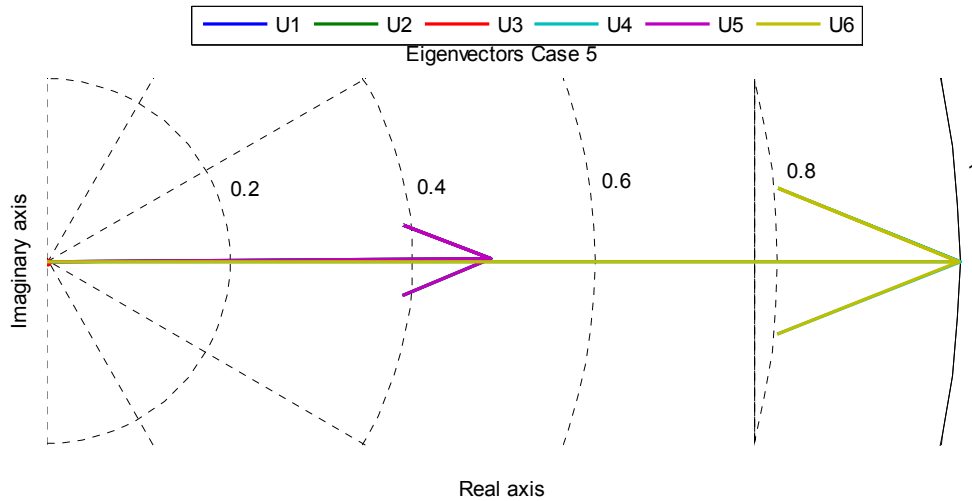


FIGURE 65: Eigenvectors case 5

6.7 Case 6 modelling

Case 6 modelling is basically the same model as case 1, with a 3-phase short circuit in the transmission line Berlin-15 de Septiembre, but there have been changes in infinite bus values. Infinite bus has a three-phase short circuit level of 2759.56 MVA and a X/R ratio of 5.25 for case 1, but for case 6 we are doing the simulation with a weak network of 2000 MVA of short circuit level, X/R ratio is the same. The fault occurs at 75 seconds and the circuit breakers operate at 75.1 seconds. The total simulation time is 120 seconds. Figure 66 shows the complete system modelling in Simulink for case 6.

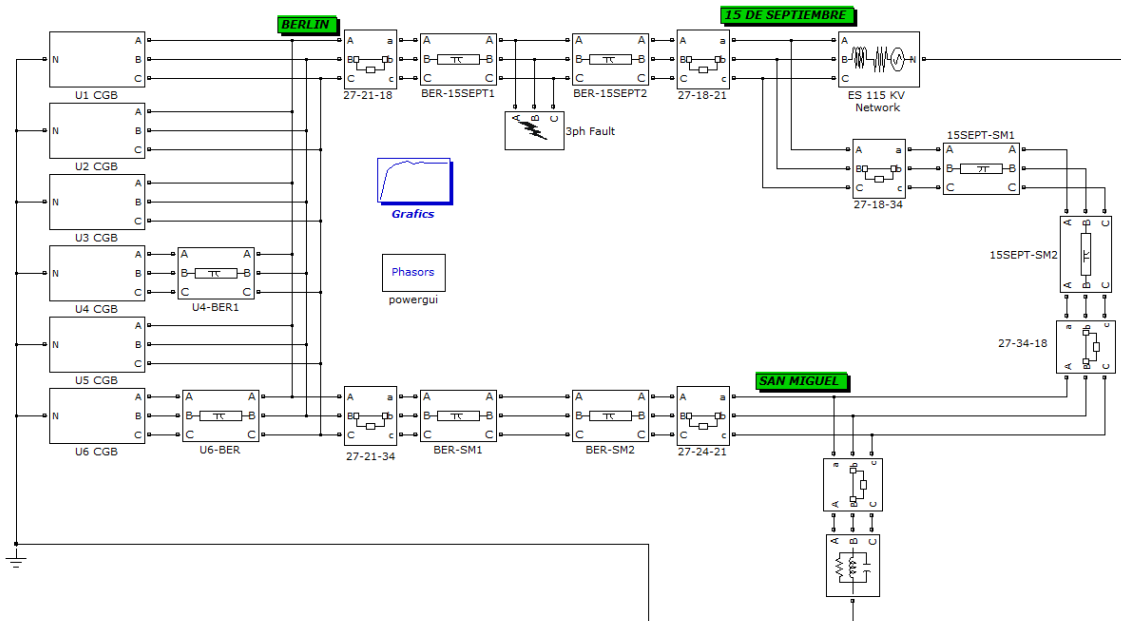


FIGURE 66: CGB case 6 modelling in Simulink

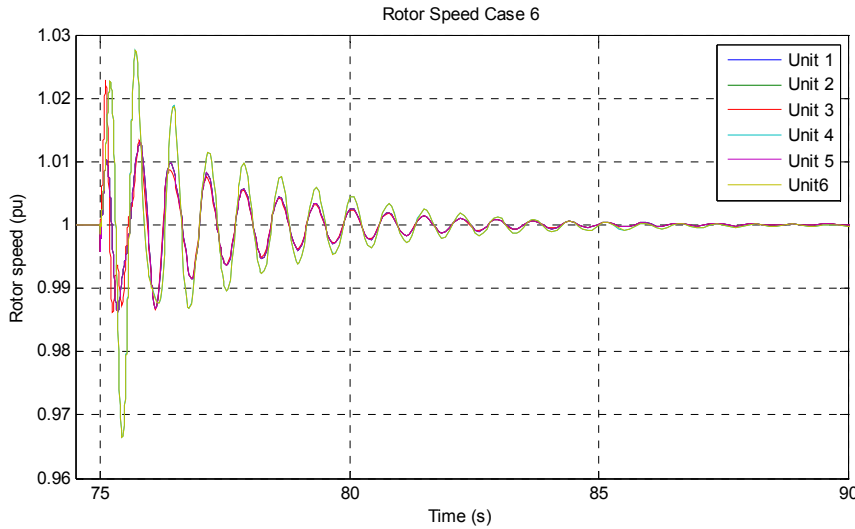


FIGURE 67: Rotor speed CGB case 6

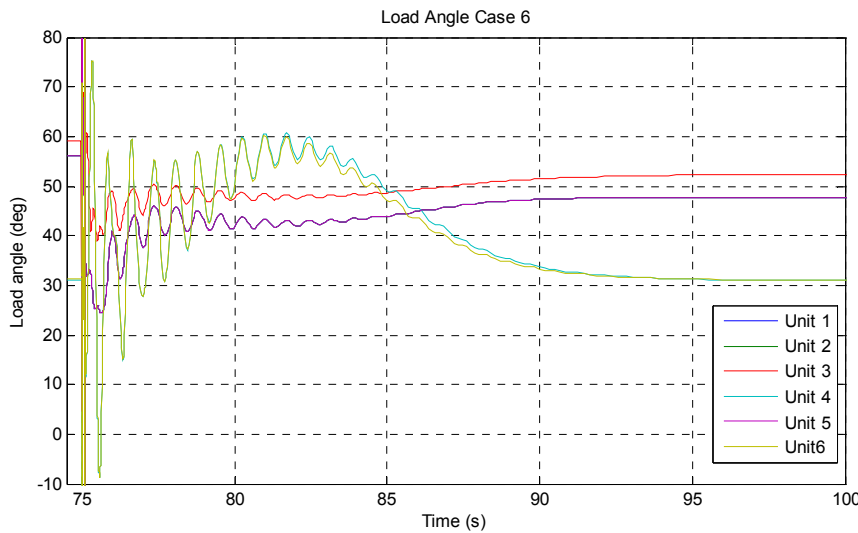


FIGURE 68: Load angle CGB case 6

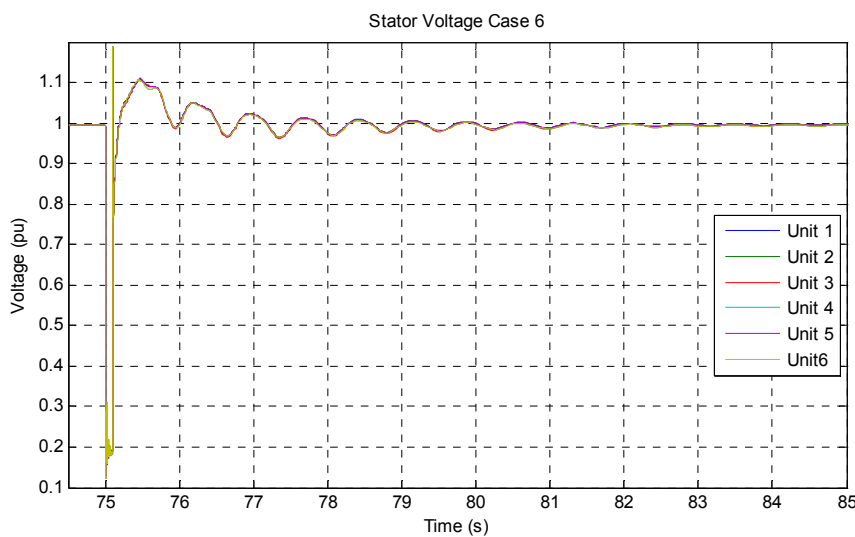


FIGURE 69: Stator voltage CGB case 6

6.7.1 Rotor speed

Figure 67 shows the rotor speed during the fault for case 6. Behaviour is very similar to case 1, with the highest oscillation at unit 4 and unit 6, maximum deviation of 0.034 pu. Oscillations have high frequency and peak values are a little higher in some cases. It takes approximately 10 seconds after the fault occurrence to return to a steady state.

6.7.2 Load angle

Figure 68 shows the load angle plot before, during and after the fault. It can be seen in the plots that changes in infinite bus produce changes in load angle before the fault. For unit 1, unit 2 and unit 5 the load angle is 56.03° , for unit 3 is 59.18° and for units 4 and unit 6 is 31.17° . After the fault, for a steady state condition, the load angle for unit 1, unit 2 and unit 5 is 47.68° , for unit 3 is 52.38° and for unit 4 and unit 5 is 31.07° .

6.7.3 Stator voltage

Figure 69 shows the behaviour of stator voltage during the fault for case 6. Behaviour is very similar to case 1, voltage collapse close to 0.1 pu during the fault, with little high oscillation peak values. Figure 70 makes a closer view of the stator voltage showing 3-phase SC effect and, after 75.1 seconds, circuit breakers operation effect.

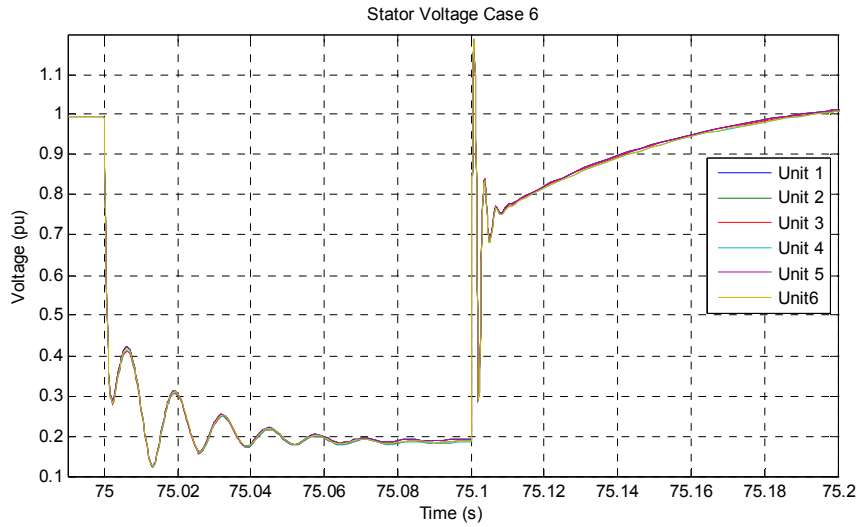


FIGURE 70: Stator voltage during fault occurrence for case 6

6.7.4 Eigenvalues and eigenvectors

Table 10 shows the eigenvalues and normalized eigenvectors for case 6 and Figure 71 shows the eigenvectors plot. In general, compared with case 1, damping values are very similar except for unit 3, frequencies are smaller for case 5. Eigenvectors magnitudes are bigger and all angles are negatives. All damping ratios are similar, except for unit 3 that is smaller.

TABLE 10: Eigenvalues, eigenvectors, frequency and damping ratio for case 6

Generator	Eigenvalues		Eigenvector		Frequency (Hz)	Damping ratio	Decay time (s)
	σ	ω	Magnitude	Angle ($^{\circ}$)			
Unit 1	-0.52	5.4	0.5	-0.97	0.86	0.096	1.92
Unit 2	-0.52	5.4	0.5	-0.97	0.86	0.096	1.92
Unit 3	-0.51	5.34	0.473	-1.094	0.85	0.095	1.96
Unit 4	-0.72	5.78	1	0	0.92	0.124	1.39
Unit 5	-0.52	5.4	0.5	-0.97	0.86	0.096	1.92
Unit 6	-0.73	5.78	1	0.003	0.92	0.125	1.37

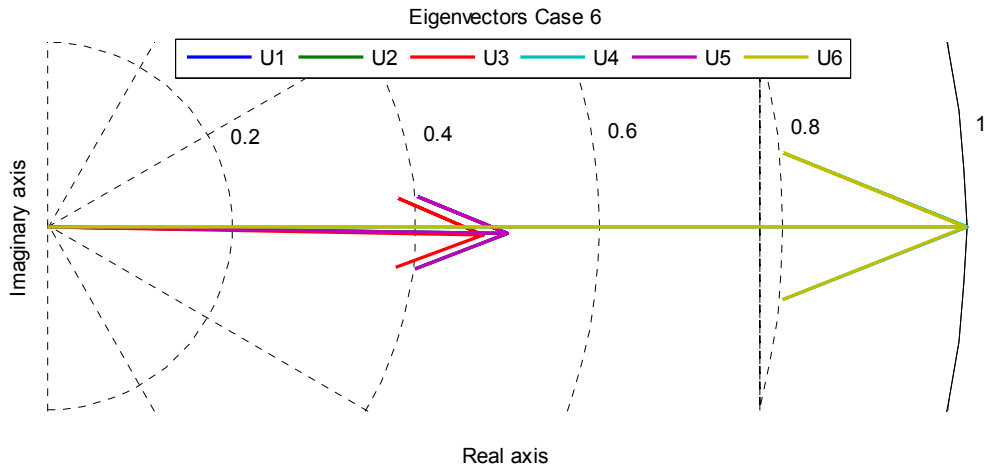


FIGURE 71: Eigenvectors case 6

7. CONCLUSIONS

This project presents a flexible model of the CGB and the surrounding grid, and it can be extended to add more units in the surroundings to make dynamics studies. The model is more flexible than other software like PSS/E, where made changes in parameters or including the model is more complicated.

Eigenvectors plots shows that the oscillation mode for our case of study is local mode or Machine system mode, because all the units of CGB swing together with respect to the rest of the power system. By extending the model (i.e. including more of the surrounding grid and other power plants) we assume that we would get additional oscillation modes, such as inter-area modes. The developed model is, however, very well suited for studying local phenomena.

During transient period, when the configuration of the system changes, the system seeks to regain stability at a new operation point, causing changes in load angles of the generators.

There is an inverse relation between damping values and damping ratio, as highest damping values, lowest damping ratio. It means that for a low damping value the rate of decay of the amplitude of the oscillation (damping ratio) will be low too, giving a high decay time for the oscillation.

The case that has the worst effect in terms of power system stability are when the short circuit is located in the line Berlin-15 de Septiembre, that correspond to case 1, case 5 and case 6. The worst of cases is the case 1, which will be taken as the reference for comparison effects.

Transmission line Berlin-15 de Septiembre is more loaded than the others transmission lines part of this study, this condition causes that the effect of the SC in the stability of the system was worst for these cases. Inherent stability criteria for case 1 show that all load angles differences are below 90° , it means that there is inherent stability with respect to unit 3.

Case 1, case 5 and case 6 present the biggest stator decrease voltage during the fault, which confirms that they are the cases that most affect the stability of CGB. Case 2 and case 3 present a considerable stator voltage reduction during the fault too, but not as severe as case 1, case 5 and case 6. Case 4 causes a very low effect in stator voltage.

Small signal stability occurs continually on the system because of small variations in load and generation. Case 4 is a small signal stability disturbance and shows that the effects of this kind of disturbances in the system are very small compared with transient stability disturbances.

Case 2 has a highest damping ratio than case 1. It means that time to decay to 37% of initial amplitude of oscillation will be smaller for all units in case 2. On the other hand, case 3 has smallest damping ratio for unit 1, unit 2, unit 3 and unit 5. It means that unit 4 and unit 6 have lowest decay time despite having the highest oscillation magnitudes.

Case 5 damping values are very similar for all units, but unit 4 and unit 6 have high damping values compared with case 1. Frequencies of oscillation are smaller for all units compared to case 1 and eigenvectors magnitudes are smaller too. This shows that in absence of unit 3, same short circuit type in line Berlin-15 de Septiembre causes a weak effect in instability of the system.

Case 6 presents a weak network, caused by the reduction in short circuit level in the infinite bus. The degree of influence on the oscillation for all units in case 6 is bigger with respect to case 1. However, the time delay on unit 4 and unit 6 is smaller for this case.

The units with the smallest damping ratio are unit 4 and unit 6 in all cases; it means that for these units decay time to reach stable state again is bigger compared with all the other units. Unit 4 and unit 6 have highest degree of influence on oscillation too, because they have the highest eigenvector magnitude for all cases.

All cases present big oscillations during the fault occurrence, and tend to return to a steady state after the circuit breakers operation. After reaching a steady state again, there have been changes in load angles, been the biggest one of 9.18° for unit 1, unit 2 and unit 5 in case 1. But, for unit 4 and unit 6 there have been no changes practically. This is because unit 4 and unit 6 return to the pre-fault operation point in the post fault period. The rest of the unit changes operation point from Pre-fault to Post-fault condition, as described in 4.7.2.

Loss of the transmission line causes a small change in load angle because of a change in impedances of the network, but the biggest influence in the load angle is because of change of operating point for unit 1, unit 2, unit 3 and unit 5. There are practically no changes in load angles for unit 4 and unit 6, related basically with changes in the impedances of the network caused by loss of transmission line or load changes.

Excitation system AC1A increases the field voltage to respond to fault condition, but in post-fault condition field voltages are not decreased, causing a change in reactive power output of each generator. Excitation system DECS-200 increase field voltage to respond to fault condition too, but it is decreased for post-fault condition, causing no changes in reactive power, as shown in Figures 72 and 73.

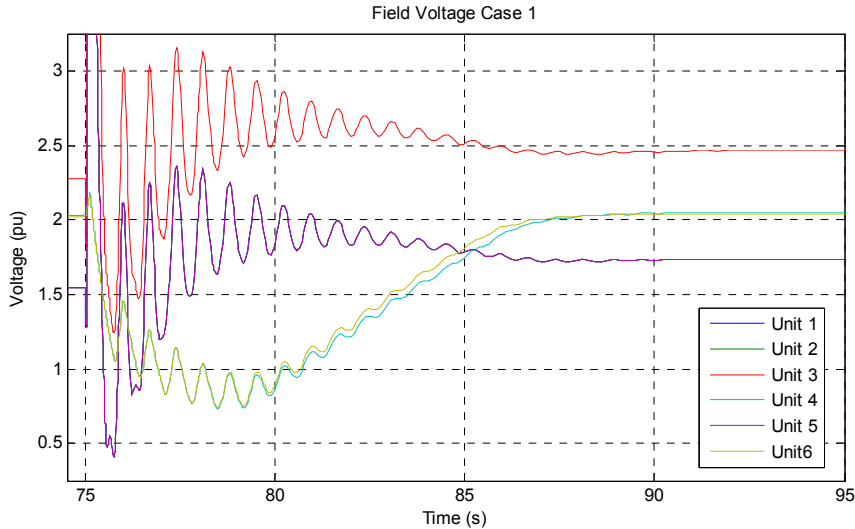


FIGURE 72: Field voltage CGB case 1

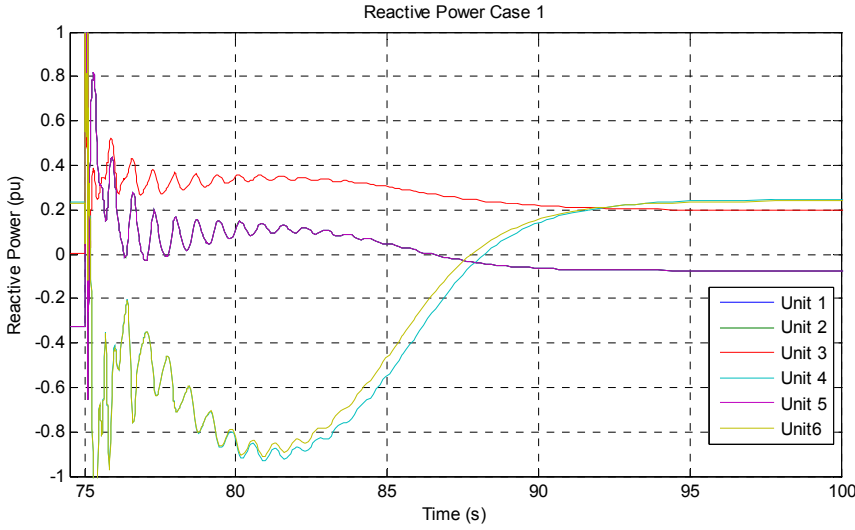


FIGURE 73: Reactive power CGB case 1

REFERENCES

- Bertani, R., 2010: Geothermal power generation in the world, 2005-2010 update report. *Proceedings of the World Geothermal Congress 2010, Bali, Indonesia*, 41 pp.
- Bonato, B.D., and Dommel, H.W., 2002: A circuit approach for the computer modelling of control transfer functions. *Proceedings of the 14th PSCC, Sevilla*, 24-28 June.
- ETESAL, 2015: *Transmission system data base 2015*. Empresa Transmisora de El Salvador, S.A. de C.V.
- Fridleifsson, I.B., and Haraldsson, I.G., 2011: Geothermal energy in the world with special reference to Central America. *Short Course of Geothermal Drilling, Resource Development and power plants, organized by UNU-GTP and LaGeo in Santa Tecla, El Salvador*, 7 pp.
- Guidos, J., and Burgos, J., 2012: Geothermal activity and development in El Salvador - producing and developing. *Short Course on Geothermal Development and Geothermal Wells*, organized by UNU-GTP and LaGeo, in Santa Tecla, El Salvador, 12 pp.
- Hauer, J.F., Demeure, C.J., Scharf, L.L., 1990: Initial results in prony analysis of power system response signals. *IEEE Transactions on Power Systems*, 5-1, 80-89.
- IEEE, 1992: *IEEE recommended practice for excitation system models for power system stability studies*. IEEE Std 421.5-1992.
- Kundur, P., 1994: *Power system stability and control*. McGraw-Hill, Inc., 1197 pp.
- Kundur, P., Paserba, J., Ajarapu, V., et al., 2003: *Definition and classification of power system stability*. IEEE/CIGRE Joint Task Force on Stability Terms and Definitions.
- Ong, Chee-Mun, 1998: *Dynamic simulation of electric machinery using Matlab/Simulink*. Prentice Hall PTR. 626 pp.
- Siemens, 2012: *PSS[®]E 33.2 Program application guide*. Siemens, July.
- Simulink, 2002: *SimPowerSystems for use with Simulink, user guide version 2*. Hydro-Québec TransÉnergie Technologies.
- Simulink, 2010: *Simulink 7 user's guide*. Webpage: www.mathworks.com
- SIGET, 2011: Bulletin on electrical statistics (in Spanish), 13, 2011. SIGET, Gerencia de Electricidad, San Salvador.
- UT, 2013: *Technical data base 2013*. Unidad de Transacciones S.A. de C.V., webpage: www.ut.com.sv.
- Valdimarson, P., 2011: Geothermal power plant cycles and main components. *Short Course on Geothermal Drilling, Resource Development and power plants, organized by UNU-GTP and LaGeo in Santa Tecla, El Salvador*, 24 pp.

APPENDIX A: Matlab code for base case plots

```
h=figure(1);
%ALL UNITS
%Governor
plot(governor_u1(:,1),governor_u1(:,3),...
     governor_u2(:,1),governor_u2(:,3),...
     governor_u3(:,1),governor_u3(:,3),...
     governor_u4(:,1),governor_u4(:,3),...
     governor_u5(:,1),governor_u5(:,3),...
     governor_u6(:,1),governor_u6(:,3));
title('Governor Output Base Case');
xlabel('Time (s)');
ylabel('Mechanical power (pu)');
legend('Unit 1','Unit 2','Unit 3','Unit 4','Unit 5','Unit6');
grid on;
saveas(h,'governor_bcbase');

%field voltage
plot(excitation_u1(:,1),excitation_u1(:,2),...
     excitation_u2(:,1),excitation_u2(:,2),...
     excitation_u3(:,1),excitation_u3(:,2),...
     excitation_u4(:,1),excitation_u4(:,2),...
     excitation_u5(:,1),excitation_u5(:,2),...
     excitation_u6(:,1),excitation_u6(:,2));
title('Field Voltage Base Case');
xlabel('Time (s)');
ylabel('Voltage (pu)');
legend('Unit 1','Unit 2','Unit 3','Unit 4','Unit 5','Unit6');
grid on;
saveas(h,'field_voltage_bcbase');

%stator voltage
plot(excitation_u1(:,1),excitation_u1(:,3),...
     excitation_u2(:,1),excitation_u2(:,3),...
     excitation_u3(:,1),excitation_u3(:,3),...
     excitation_u4(:,1),excitation_u4(:,3),...
     excitation_u5(:,1),excitation_u5(:,3),...
     excitation_u6(:,1),excitation_u6(:,3));
title('Stator Voltage Base Case');
xlabel('Time (s)');
ylabel('Voltage (pu)');
legend('Unit 1','Unit 2','Unit 3','Unit 4','Unit 5','Unit6');
grid on;
saveas(h,'stator_voltage_bcbase');

%rotor speed
plot(rotor_speed_u1(:,1),rotor_speed_u1(:,2),...
     rotor_speed_u2(:,1),rotor_speed_u2(:,2),...
     rotor_speed_u3(:,1),rotor_speed_u3(:,2),...
     rotor_speed_u4(:,1),rotor_speed_u4(:,2),...
     rotor_speed_u5(:,1),rotor_speed_u5(:,2),...
     rotor_speed_u6(:,1),rotor_speed_u6(:,2));
title('Rotor Speed Base Case');
xlabel('Time (s)');
ylabel('Rotor speed (pu)');
```

```

legend('Unit 1','Unit 2','Unit 3','Unit 4','Unit 5','Unit6');
grid on;
saveas(h,'rotor_speed_bcase');

%Load angle
plot(load_angle_u1(:,1),load_angle_u1(:,2),...
     load_angle_u2(:,1),load_angle_u2(:,2),...
     load_angle_u3(:,1),load_angle_u3(:,2),...
     load_angle_u4(:,1),load_angle_u4(:,2),...
     load_angle_u5(:,1),load_angle_u5(:,2),...
     load_angle_u6(:,1),load_angle_u6(:,2));
title('Load Angle Base Case');
xlabel('Time (s)');
ylabel('Load angle (deg)');
legend('Unit 1','Unit 2','Unit 3','Unit 4','Unit 5','Unit6');
grid on;
saveas(h,'load_angle_bcase');

%Active power
plot(power_u1(:,1),power_u1(:,2),...
     power_u2(:,1),power_u2(:,2),...
     power_u3(:,1),power_u3(:,2),...
     power_u4(:,1),power_u4(:,2),...
     power_u5(:,1),power_u5(:,2),...
     power_u6(:,1),power_u6(:,2));
title('Active Power Base Case');
xlabel('Time (s)');
ylabel('Active Power (pu)');
legend('Unit 1','Unit 2','Unit 3','Unit 4','Unit 5','Unit6');
grid on;
saveas(h,'active_power_bcase');

%Reactive power
plot(power_u1(:,1),power_u1(:,3),...
     power_u2(:,1),power_u2(:,3),...
     power_u3(:,1),power_u3(:,3),...
     power_u4(:,1),power_u4(:,3),...
     power_u5(:,1),power_u5(:,3),...
     power_u6(:,1),power_u6(:,3));
title('Reactive Power Base Case');
xlabel('Time (s)');
ylabel('Reactive Power (pu)');
legend('Unit 1','Unit 2','Unit 3','Unit 4','Unit 5','Unit6');
grid on;
saveas(h,'reactive_power_bcase');

close all
save 'base_case'
clear
clc

```

APPENDIX B: Typical Matlab code for case 1 to case 6 plots

```
h=figure(1);
%ALL UNITS
%Governor
plot(governor_u1_case1(:,1),governor_u1_case1(:,3),...
     governor_u2_case1(:,1),governor_u2_case1(:,3),...
     governor_u3_case1(:,1),governor_u3_case1(:,3),...
     governor_u4_case1(:,1),governor_u4_case1(:,3),...
     governor_u5_case1(:,1),governor_u5_case1(:,3),...
     governor_u6_case1(:,1),governor_u6_case1(:,3));
title('Governor Output Case 1');
xlabel('Time (s)');
ylabel('Mechanical power (pu)');
legend('Unit 1','Unit 2','Unit 3','Unit 4','Unit 5','Unit6');
grid on;
saveas(h,'governor_case1');

%field voltage
plot(excitation_u1_case1(:,1),excitation_u1_case1(:,2),...
     excitation_u2_case1(:,1),excitation_u2_case1(:,2),...
     excitation_u3_case1(:,1),excitation_u3_case1(:,2),...
     excitation_u4_case1(:,1),excitation_u4_case1(:,2),...
     excitation_u5_case1(:,1),excitation_u5_case1(:,2),...
     excitation_u6_case1(:,1),excitation_u6_case1(:,2));
title('Field Voltage Case 1');
xlabel('Time (s)');
ylabel('Voltage (pu)');
legend('Unit 1','Unit 2','Unit 3','Unit 4','Unit 5','Unit6');
grid on;
saveas(h,'field_voltage_case1');

%stator voltage
plot(excitation_u1_case1(:,1),excitation_u1_case1(:,3),...
     excitation_u2_case1(:,1),excitation_u2_case1(:,3),...
     excitation_u3_case1(:,1),excitation_u3_case1(:,3),...
     excitation_u4_case1(:,1),excitation_u4_case1(:,3),...
     excitation_u5_case1(:,1),excitation_u5_case1(:,3),...
     excitation_u6_case1(:,1),excitation_u6_case1(:,3));
title('Stator Voltage Case 1');
xlabel('Time (s)');
ylabel('Voltage (pu)');
legend('Unit 1','Unit 2','Unit 3','Unit 4','Unit 5','Unit6');
grid on;
saveas(h,'stator_voltage_case1');

%rotor speed
plot(rotor_speed_u1_case1(:,1),rotor_speed_u1_case1(:,2),...
     rotor_speed_u2_case1(:,1),rotor_speed_u2_case1(:,2),...
     rotor_speed_u3_case1(:,1),rotor_speed_u3_case1(:,2),...
     rotor_speed_u4_case1(:,1),rotor_speed_u4_case1(:,2),...
     rotor_speed_u5_case1(:,1),rotor_speed_u5_case1(:,2),...
     rotor_speed_u6_case1(:,1),rotor_speed_u6_case1(:,2));
title('Rotor Speed Case 1');
xlabel('Time (s)');
ylabel('Rotor speed (pu)');
```

```

legend('Unit 1','Unit 2','Unit 3','Unit 4','Unit 5','Unit6');
grid on;
saveas(h,'rotor_speed_case1');

%Load angle
plot(load_angle_u1_case1(:,1),load_angle_u1_case1(:,2),...
      load_angle_u2_case1(:,1),load_angle_u2_case1(:,2),...
      load_angle_u3_case1(:,1),load_angle_u3_case1(:,2),...
      load_angle_u4_case1(:,1),load_angle_u4_case1(:,2),...
      load_angle_u5_case1(:,1),load_angle_u5_case1(:,2),...
      load_angle_u6_case1(:,1),load_angle_u6_case1(:,2));
title('Load Angle Case 1');
xlabel('Time (s)');
ylabel('Load angle (deg)');
legend('Unit 1','Unit 2','Unit 3','Unit 4','Unit 5','Unit6');
grid on;
saveas(h,'load_angle_case1');

%Active power
plot(power_u1_case1(:,1),power_u1_case1(:,2),...
      power_u2_case1(:,1),power_u2_case1(:,2),...
      power_u3_case1(:,1),power_u3_case1(:,2),...
      power_u4_case1(:,1),power_u4_case1(:,2),...
      power_u5_case1(:,1),power_u5_case1(:,2),...
      power_u6_case1(:,1),power_u6_case1(:,2));
title('Active Power Case 1');
xlabel('Time (s)');
ylabel('Active Power (pu)');
legend('Unit 1','Unit 2','Unit 3','Unit 4','Unit 5','Unit6');
grid on;
saveas(h,'active_power_case1');

%Reactive power
plot(power_u1_case1(:,1),power_u1_case1(:,3),...
      power_u2_case1(:,1),power_u2_case1(:,3),...
      power_u3_case1(:,1),power_u3_case1(:,3),...
      power_u4_case1(:,1),power_u4_case1(:,3),...
      power_u5_case1(:,1),power_u5_case1(:,3),...
      power_u6_case1(:,1),power_u6_case1(:,3));
title('Reactive Power Case 1');
xlabel('Time (s)');
ylabel('Reactive Power (pu)');
legend('Unit 1','Unit 2','Unit 3','Unit 4','Unit 5','Unit6');
grid on;
saveas(h,'reactive_power_case1');

close all
save CGB_case1
clear
clc

```

APPENDIX C: Matlab code for eigenvectors plots and damping factor calculation

```
a=cell2mat([poles_case1',poles_case2',poles_case3',...
poles_case4',poles_case5',poles_case6']);

%Unit in rows and cases in columns
for m=1:6 %calculate damping factor
for n=1:6
damping_ratio(m,n)=-eigenvalues(m,n*2-1)/...
sqrt(eigenvalues(m,n*2-1)^2+eigenvalues(m,n*2)^2);
end
end
for m=1:6
for n=1:6
if imag(a(m,n)) < 0; %get positives poles values
CGB_poles_allcases(m,n)=conj((a(m,n)));
else CGB_poles_allcases(m,n)=(a(m,n));
end
end
end
for m=1:6
for n=1:6
eigenvectors_angles(m,n)=angle(CGB_poles_allcases(m,n)); %gets angles of poles to eigenvector
angles in rad
end
end
[value,row]=max(eigenvectors_abs); %gets max value and position to normalize eigenvectors
for m=1:6
b(1,m)=eigenvectors_abs(row(m),m); %gets reference vector to normalize magnitude
c(1,m)=eigenvectors_angles(row(m),m); %gets reference vector to normalize angle
end
norm_abs=[b;b;b;b;b];
norm_ang=[c;c;c;c;c];
eigenvectors_abs_norm=eigenvectors_abs./norm_abs; %normalized magnitudes
eigenvectors_angles_norm=eigenvectors_angles-norm_ang;%normalized angles
eigenvectors_angles_deg=rad2deg(eigenvectors_angles);%convert rad to deg in eigenvectors angles
eigenvectors_angles_norm_deg=rad2deg(eigenvectors_angles_norm);%conver rad to deg in
eigenvectors angles normalized
for m=1:6
for n=1:6
[x(m,n),y(m,n)]=pol2cart(eigenvectors_angles_norm(m,n),...
eigenvectors_abs_norm(m,n)); %converts polar to rectangular coordenates
eigenvectors(m,n)=x(m,n)+y(m,n)*1i;
end
end

case1=eigenvectors(:,1);
case2=eigenvectors(:,2);
case3=eigenvectors(:,3);
case4=eigenvectors(:,4);
case5=eigenvectors(:,5);
case6=eigenvectors(:,6);

%CASE1
f=figure(1);
clr = lines(numel(case1)); %colors you want to use
```

```

h = compass(case1);      %compass(real(Z),imag(Z))
set(h, {'Color'},num2cell(clr,2), 'LineWidth',2)
str = cellstr( num2str((1:numel(case1)),'U%d' ) );
legend(h, str, 'Location','BestOutside')
xlabel('Real axis');
ylabel('Imaginary axis');
title('Eigenvectors Case 1');
saveas(f,'eigenvectors_case1');

%CASE2
f=figure(2);
clr = lines(numel(case2)); %colors you want to use
h = compass(case2);      %compass(real(Z),imag(Z))
set(h, {'Color'},num2cell(clr,2), 'LineWidth',2)
str = cellstr( num2str((1:numel(case2)),'U%d' ) );
legend(h, str, 'Location','BestOutside')
xlabel('Real axis');
ylabel('Imaginary axis');
title('Eigenvectors Case 2');
saveas(f,'eigenvectors_case2');

%CASE3
f=figure(3);
clr = lines(numel(case3)); %colors you want to use
h = compass(case3);      %compass(real(Z),imag(Z))
set(h, {'Color'},num2cell(clr,2), 'LineWidth',2)
str = cellstr( num2str((1:numel(case3)),'U%d' ) );
legend(h, str, 'Location','BestOutside')
xlabel('Real axis');
ylabel('Imaginary axis');
title('Eigenvectors Case 3');
saveas(f,'eigenvectors_case3');

%CASE4
f=figure(4);
clr = lines(numel(case4)); %colors you want to use
h = compass(case4);      %compass(real(Z),imag(Z))
set(h, {'Color'},num2cell(clr,2), 'LineWidth',2)
str = cellstr( num2str((1:numel(case4)),'U%d' ) );
legend(h, str, 'Location','BestOutside')
xlabel('Real axis');
ylabel('Imaginary axis');
title('Eigenvectors Case 4');
saveas(f,'eigenvectors_case4');

%CASE5
f=figure(5);
clr = lines(numel(case5)); %colors you want to use
h = compass(case5);      %compass(real(Z),imag(Z))
set(h, {'Color'},num2cell(clr,2), 'LineWidth',2)
str = cellstr( num2str((1:numel(case5)),'U%d' ) );
legend(h, str, 'Location','BestOutside')
xlabel('Real axis');
ylabel('Imaginary axis');
title('Eigenvectors Case 5');
saveas(f,'eigenvectors_case5');

```

```
%CASE6
f=figure(6);
clr = lines(numel(case6)); %colors you want to use
h = compass(case6); %compass(real(Z),imag(Z))
set(h, {'Color'},num2cell(clr,2), 'LineWidth',2)
str = cellstr( num2str((1:numel(case6)),'U%d' ) );
legend(h, str, 'Location','BestOutside')
xlabel('Real axis');
ylabel('Imaginary axis');
title('Eigenvectors Case 6');
saveas(f,'eigenvectors_case6');

close all
save eigenvectors_and_damping
clear
clc
```

